

NBSIR 86-3467

A11102 631302

NAT'L INST OF STANDARDS & TECH R.I.C.



A11102631302

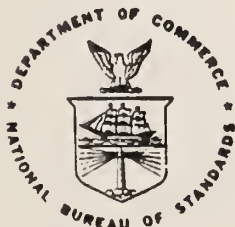
Gaynor, Patricia/Influence of mortar bed
QC100 .U58 NO.88-3467 1987 V19 C.1 NBS-P

Influence of Mortar Bedding on Prism Behavior

Patricia Gaynor
Kyle Woodward
Charles Scribner

U.S. DEPARTMENT OF COMMERCE
National Bureau of Standards
National Engineering Laboratory
Center for Building Technology
Gaithersburg, MD 20899

February 1987



U.S. DEPARTMENT OF COMMERCE
NATIONAL BUREAU OF STANDARDS

QC

100

.U56

86-3467

1987

c.2

11BSC

QC100

.456

10.86-3467

1987

C.2

NBSIR 86-3467

**INFLUENCE OF MORTAR BEDDING ON
MASONRY PRISM BEHAVIOR**

Patricia Gaynor
Kyle Woodward
Charles Scribner

U.S. DEPARTMENT OF COMMERCE
National Bureau of Standards
National Engineering Laboratory
Center for Building Technology
Gaithersburg, MD 20899

February 1987

U.S. DEPARTMENT OF COMMERCE, Malcolm Baldrige, *Secretary*
NATIONAL BUREAU OF STANDARDS, Ernest Ambler, *Director*

ABSTRACT

The results from compression tests of seventy ungrouted, hollow concrete block masonry prisms are presented. The prisms are three-unit high, stack-bonded assemblages. The parameters varied in the investigation include block strength, mortar type, and mortar bedding type (area). The resulting data include the compressive strengths of the prisms and strains measured at various locations on each prism. Major observations of prism behavior are that mortar type has a negligible influence on prism behavior, block strength affects masonry prism strength in proportion to its own variation, and mortar bedding type significantly affects masonry prism strength, variability of strength, strain distributions, and mode of failure. It is shown that disturbed strain fields occur in faceshell-bedded prisms and that the variability of data obtained from tests of faceshell-bedded prisms is high. For these reasons, it is recommended that fully-bedded prisms be used as quality control samples for masonry construction.

TABLE OF CONTENTS

	<u>Page</u>
ABSTRACT	ii
LIST OF TABLES	iv
LIST OF FIGURES	v
1. INTRODUCTION	1
2. TEST SPECIMENS	2
2.1 MATERIALS	2
2.2 PRISM DETAILS AND TESTING	2
3. MASONRY PRISM STRENGTH ANALYSIS	12
3.1 MODES OF FAILURE	12
3.2 EFFECT OF BEDDING TYPE	16
3.3 EFFECT OF MORTAR STRENGTH	19
3.4 EFFECT OF BLOCK STRENGTH	19
4. PRISM STRAIN DISTRIBUTION	21
4.1 UNIFORMITY OF STRAIN	21
4.1.1 Full-Area-Bedded Prisms	21
4.1.2 Faceshell-Bedded Prisms	21
4.2 MODE OF FAILURE AND WEB STRAINS	26
4.2.1 Faceshell-Bedded Prisms	26
4.2.2 Full-Area-Bedded Prisms	33
4.2.3 Influence of Mortar Bedding	33
4.3 STRAIN REDISTRIBUTION DUE TO WEB SPLITTING ...	36
5. IMPLICATIONS OF RESULTS	38
5.1 COMPRESSIVE STRENGTH AND ITS VARIABILITY	38
5.1.1 Compressive Strength	38
5.1.2 Variability of Compressive Strength ...	39
5.2 STRAIN DISTRIBUTION	41
5.3 RECOMMENDATION	41
6. SUMMARY AND CONCLUSIONS	43
6.1 SUMMARY	43
6.2 CONCLUSIONS	43
7. ACKNOWLEDGMENTS	44
8. REFERENCES	45
APPENDICES	
A. FINITE ELEMENT MODEL	46
A.1 MODEL	46
A.2 ANALYSIS	46
A.2.1 Full-Area-Bedded Prisms	46
A.2.2 Faceshell-Bedded Prisms	50
B. PRISM UNIAXIAL STRESS-STRAIN CURVES	53

LIST OF TABLES

	<u>Page</u>
Table 2.1 Details of Masonry Units	4
Table 2.2 Mortar 28-day Compressive Strengths	5
Table 3.1 Faceshell-Bedded Masonry Prism Compressive Strength	13
Table 3.2 Full-Area-Bedded Masonry Prism Compressive Strength	14
Table 3.3 Ratio of Average Compressive Strengths Faceshell to Full-Area Bedding	18
Table 3.4 Average Compressive Strengths by Group	18
Table 3.5 Coefficient of Variation of Compressive Strengths	20
Table 3.6 Ratio of Average Compressive Strengths Low to High Strength Mortar	20
Table 3.7 Ratio of Average Compressive Strengths Low to High Strength Block	20
Table 5.1 Average Compressive Strength Based on Mortared Area	40

LIST OF FIGURES

	<u>Page</u>
Figure 2.1 Concrete block	3
Figure 2.2 Concrete block prism	7
Figure 2.3 Mortar bedding types	7
Figure 2.4 LVDT instrumentation	8
Figure 2.5 Leaf spring transducer instrumentation	9
Figure 2.6 Locations of LST's and LVDT's	10
Figure 3.1 Failure of a full-area-bedded prism	15
Figure 3.2 Failure of a faceshell-bedded prism	17
Figure 4.1 Web vertical strain by block for full-area-bedded prisms	22
Figure 4.2 Web lateral strain by block for full-area-bedded prisms	23
Figure 4.3 Comparison of vertical strains - faceshell to web for full-area-bedded prisms	24
Figure 4.4 Comparison of faceshell vertical strain by block for full-area-bedded prisms	25
Figure 4.5 Comparison of web vertical strain by block for faceshell-bedded prisms	27
Figure 4.6 Influence of web stiffness on vertical strain distribution for faceshell-bedded prisms	28
Figure 4.7 Comparison of faceshell vertical strains by block for faceshell-bedded prisms	29
Figure 4.8 Stress trajectories in webs of a faceshell-bedded prism	31
Figure 4.9 Support conditions for webs of faceshell-bedded prisms	32
Figure 4.10 Web lateral strains by block for faceshell-bedded prisms	34
Figure 4.11 Stress trajectories in webs of a full-area-bedded prism	35
Figure 4.12 Strain redistribution after web cracking in faceshell-bedded prisms	37
Figure A.1 Finite element mesh	47
Figure A.2 Finite element prism dimensions (inches) ..	48
Figure A.3 Loading on finite element prism	49
Figure A.4 Stress trajectories in faceshell of a full-area-bedded prism	51
Figure A.5 Stress trajectories in faceshell of a faceshell-bedded prism	52

LIST OF FIGURES (continued)

		<u>Page</u>
Figure B.1	Stress-strain curves for prisms with low-strength mortar, low-strength block, and faceshell bedding	54
Figure B.2	Stress-strain curves for prisms with low-strength mortar, low-strength block, and full-area bedding	55
Figure B.3	Stress-strain curves for prisms with high-strength mortar, low-strength block, and faceshell bedding	56
Figure B.4	Stress-strain curves for prisms with high-strength mortar, low-strength block, and full-area bedding	57
Figure B.5	Stress-strain curves for prisms with low-strength mortar, high-strength block, and faceshell bedding	58
Figure B.6	Stress-strain curves for prisms with high-strength mortar, high-strength block, and faceshell bedding	59
Figure B.7	Stress-strain curves for prisms with high-strength mortar, high-strength block, and full-area bedding	60

1. INTRODUCTION

Results from uniaxial compression tests of hollow concrete block masonry prisms were investigated for this report. The prisms were constructed as companion specimens to wall panels and were tested to obtain a measure of the uniaxial compressive strength of the wall panels. The wall panels were the primary test specimens under study in the overall research program and, consequently, the prisms were not originally built with the intention of conducting a research study on their behavior. However, the instrumentation that was to be used on the wall panels was placed on the prisms to verify its operation and as a result, an extensive amount of data on the strain distributions in masonry prisms were obtained. The analysis of the data and an examination of conditions at failure produced a comprehensive description of the behavior of these masonry prisms in uniaxial compression. The analysis of the experimental data was aided by a simple but effective finite element analysis.

Compression testing of masonry prisms is typically governed by ASTM Standard E447[1]. Such tests yield a measure of the compressive strength of a masonry assemblage, typically expressed as a stress. One use of compression testing of prisms is to assure that the masonry materials used to build a structure achieve a specified design strength. The compressive strength of masonry is used in the design process to calculate a number of different allowable stresses in structural members constructed of masonry. Allowable compressive and flexural stresses, allowable bearing stress, allowable shearing stress in masonry, and the moduli of elasticity and rigidity are typically expressed as functions of the compressive strength of masonry prisms, as in ACI 531-79, Building Code Requirements for Concrete Masonry Structures[2].

In the experimental study reported herein, seventy prisms were constructed, instrumented and tested. Mortar strength, block strength and type of mortar bedding were the varied parameters. There were two types of mortar, two block unit strengths, and two types of mortar bedding. The principal data obtained from the tests were histories of the applied load and the resulting displacements (strains) at various locations on the prisms' faceshells and webs. In addition, crack patterns and failure modes were recorded.

Chapter 2 details the materials, construction and testing procedures. Experimental conditions at failure are described in Chapter 3. Chapter 4 presents a description of strain distributions based on finite element analyses and experimental results. Implications of the data are discussed in Chapter 5. A brief overview of the finite element analyses is presented in Appendix A. The uniaxial stress-strain curves for all of the prisms are shown in Appendix B.

2. TEST SPECIMENS

2.1 MATERIALS

All materials used in constructing the prisms were commercially available and were representative of those commonly used in masonry construction. The masonry units were hollow, two-core concrete blocks, as shown in figure 2.1 and described in Table 2.1. The thickness of the faceshells and the webs of the units varied along the height of the units. The concrete blocks were from one of two lots. One lot contained blocks having a gross-area unit compressive strength of 1813 psi and the other lot contained blocks with a gross-area unit compressive strength of 1304 psi. For the purposes of this report, the blocks that had the strength of 1813 psi were termed "high" strength while the blocks that had a strength of 1304 psi were termed "low" strength. These terms were used as descriptions of relative strengths and were not intended to be a classification of the absolute strengths of the blocks.

The mortar used in constructing the prisms was proportioned as either Type S, which was termed "high" strength, or Type N, which was designated "low" strength. Both mortars were proportioned in accordance with ASTM C270[3], with the Type S mortar having a ratio of cement:lime:sand of 1:3/8:4 by volume. Type N mortar was proportioned as 1:1:5 of cement:lime:sand. One wall, three prisms, and six mortar cubes were made from each batch of mortar. Mortar cubes were air cured to match the curing conditions of the prisms. After 28 days of curing, three cubes from each mortar batch were tested and their compressive strengths were averaged to obtain a measure of the mortar's compressive strength. The average measured strengths of mortars are listed in Table 2.2. The overall compressive strength was 2571 psi for the high-strength mortar and 1726 psi for the low-strength mortar. These mortars were batched and tested over a period of eight months.

2.2 PRISM DETAILS AND TESTING

One use of compression testing of prisms is to assure that the specified design strength of masonry is achieved by the masonry materials used to build a structure. When used to this end, prisms are normally constructed with the same materials and workmanship as those in the structure. Workmanship includes mortar bedding type and mortar joint tooling. However, prisms are typically laid in stack bond regardless of the bond pattern used in the structure. The usual practice is to cap prisms fully on both bearing surfaces. The strength of prisms constructed of hollow blocks is calculated by dividing the maximum load sustained by a prism by the net cross-sectional area of the blocks.

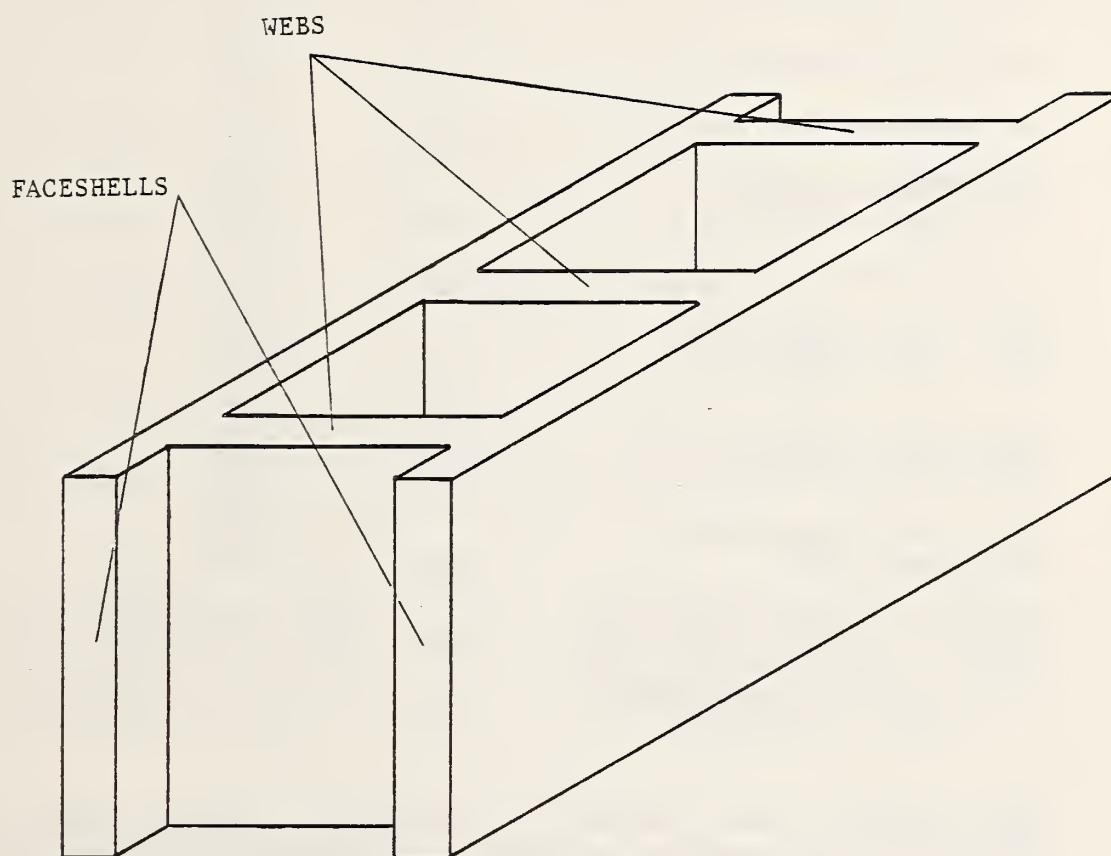


Figure 2.1 Concrete block

Table 2.1 Details of Masonry Units

	Low-Strength Unit	High-Strength Unit
Width (inches)	7.65	7.63
Height (inches)	7.56	7.59
Length (inches)	15.66	15.62
Minimum Faceshell Thickness (inches)	1.30	1.30
Gross Area (sq. in.)	119.8	119.2
Net Cross-sectional Area (sq. in.)	60.4	61.5
Gross Area Compressive Strength (psi)	1304	1813
Net Area Compressive Strength (psi)	2586	3514
Density (lb/cu. ft.)	98.1	102.4
Absorption (lb/cu. ft.)	14.0	10.8

Measurements were made in accordance with ASTM C140[4] and represent the average for six high-strength units and nine low-strength units.

Table 2.2 Mortar 28-day Compressive Strengths

<u>High-Strength Mortar</u>		<u>Low-Strength Mortar</u>	
Prism Identifier	Compressive Strength (psi) *	Prism Identifier	Compressive Strength (psi) *
3 - 1	1825	5 - 1	1826
3 - 2	2139	5 - 2	1809
3 - 3	2095	5 - 3	1761
3 - 4	2237	5 - 4	1490
3 - 5	2055	6 - 6	1841
3 - 6	1847	6 - 7	1987
4 - 1	3254	6 - 8	1591
4 - 2	2746	6 - 9	1505
4 - 3	3067		
4 - 4	2425		
6 - 1	2646		
6 - 2	2657		
6 - 3	2772		
6 - 4	3127		
6 - 10	2985		
6 - 11	2892		
6 - 12	2700		
6 - 13	2810		
<hr/> Average Stress= 2571 psi		<hr/> Average Stress= 1726 psi	
Std. Deviation= 444 psi		Std. Deviation= 178 psi	
Coefficient of		Coefficient of	
Variation= 17.3%		Variation= 10.3%	

* Each strength entry is the average of the compressive strength of three mortar cubes.

Prisms were constructed by stack bonding three stretcher units (fig. 2.2). Blocks were placed with the thicker cross-section towards the top. This convention made mortaring easier and was consistent with typical masonry construction practice. Mortar bedding was either faceshell or full-area bedding (fig. 2.3). Mortar joints were struck flush with a trowel, but were not tooled. The mason used a four-foot level to maintain the level of each block and to plumb the prism. Prisms were cured in air for at least 28 days and then fully capped. Prisms were from 90 to 185 days old when tested.

Prisms were tested in a uniaxial testing machine having a capacity of 400,000 pounds force. A spherically-seated upper bearing block covered the entire bearing area of the prism under test. The load was applied to the prism at any convenient rate for the first 40,000 pounds force while the remaining load was applied at a rate of 40,000 pounds force per minute until failure occurred. The maximum load sustained by a prism was used in computing its compressive strength.

Prisms were instrumented with two different types of displacement measuring devices. Every prism was instrumented with two linear variable differential transformers (LVDT's) oriented vertically, one on each faceshell at mid-length (fig. 2.4). The gage length of the LVDT's was sixteen inches measured between the approximate vertical centers of the top and bottom blocks. Twelve leaf spring transducers (LST's) (fig. 2.5) were placed on each prism over a gage length of either $3/4$ inch or 1 inch. The mounting location of the LST's varied between groups of prisms. Thus, while all of the mounting locations and orientations identified in figure 2.6 were used during the test program, LST's were not placed at all of the locations during the test of each prism. It was not possible to place LST's both vertically and horizontally over the same gage area. Vertical and horizontal displacement data at the same location were obtained by using separate, but comparable prisms, one instrumented to measure vertical strains and the other to measure horizontal strains. It was not possible to place LST's across LVDT gage lengths.

The displacement data and the load data from the testing machine were read simultaneously at regular intervals during a prism test. The displacement data were subsequently divided by appropriate gage lengths to produce strain data. The combination of the load and deflection data into a plot of stress vs. strain produced a strain history that described the response at the gage location for the duration of the test.

The two types of displacement sensors provided two descriptions of prism behavior. LVDT's measured deflections over a gage length that encompassed a large percentage of the height of a three-unit-high masonry prism. As a result, the LVDT data were good indicators of average prism behavior. LVDT's were placed in

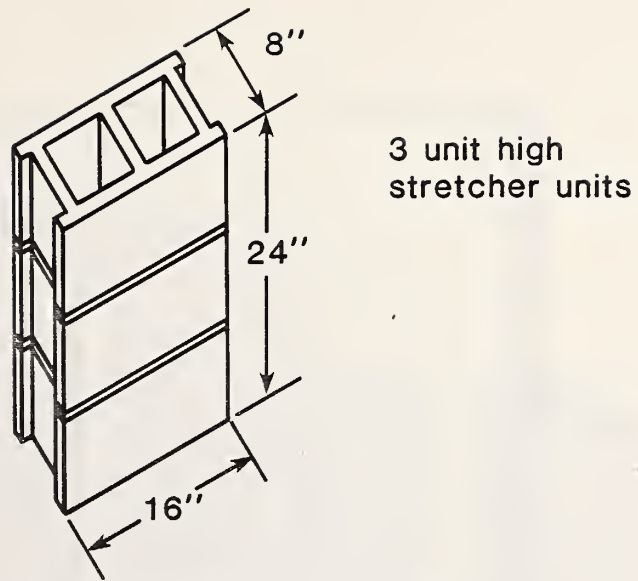


Figure 2.2 Concrete block prism

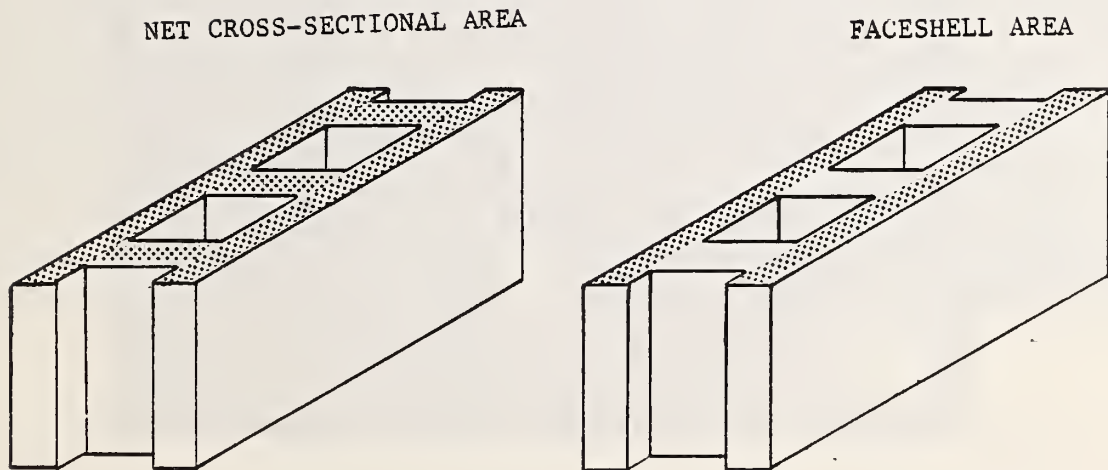


Figure 2.3 Mortar bedding types

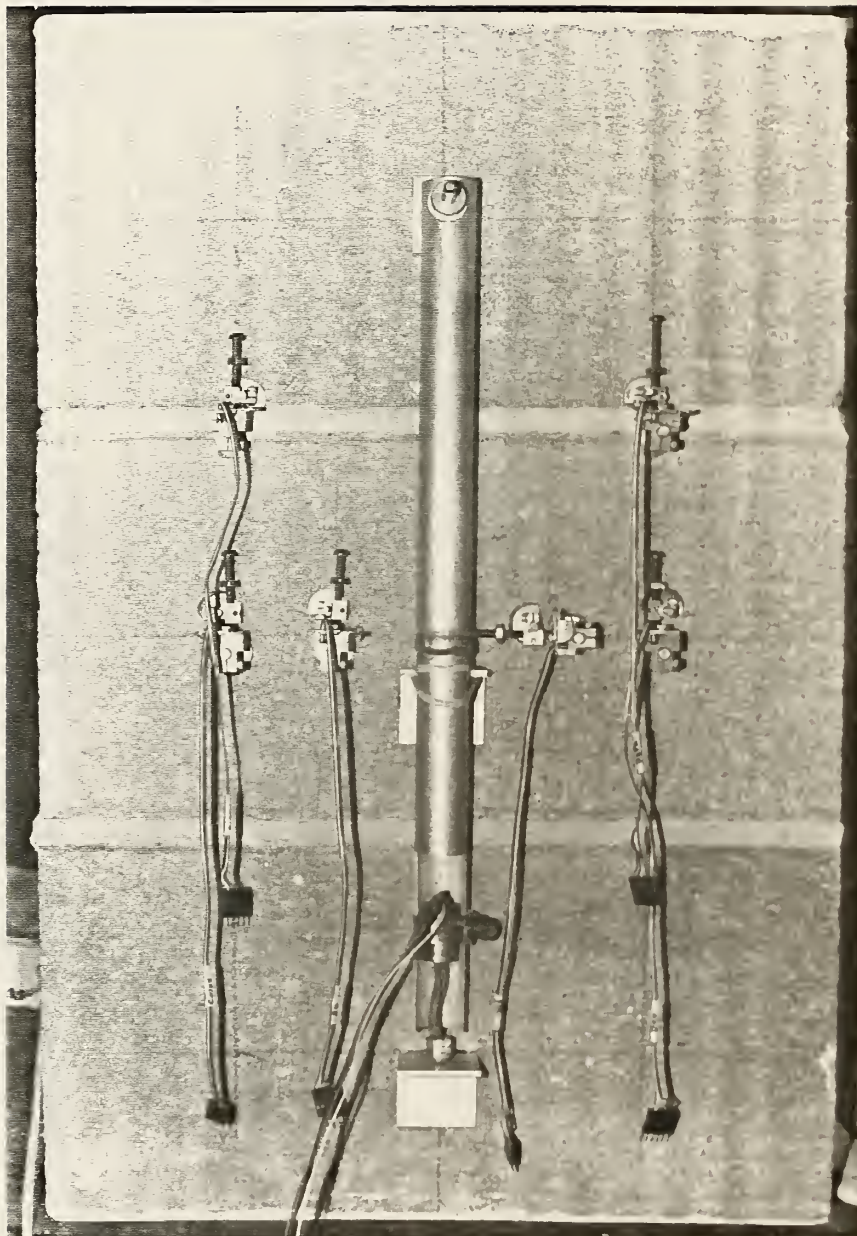


Figure 2.4 LVDT instrumentation



Figure 2.5 Leaf spring transducer instrumentation

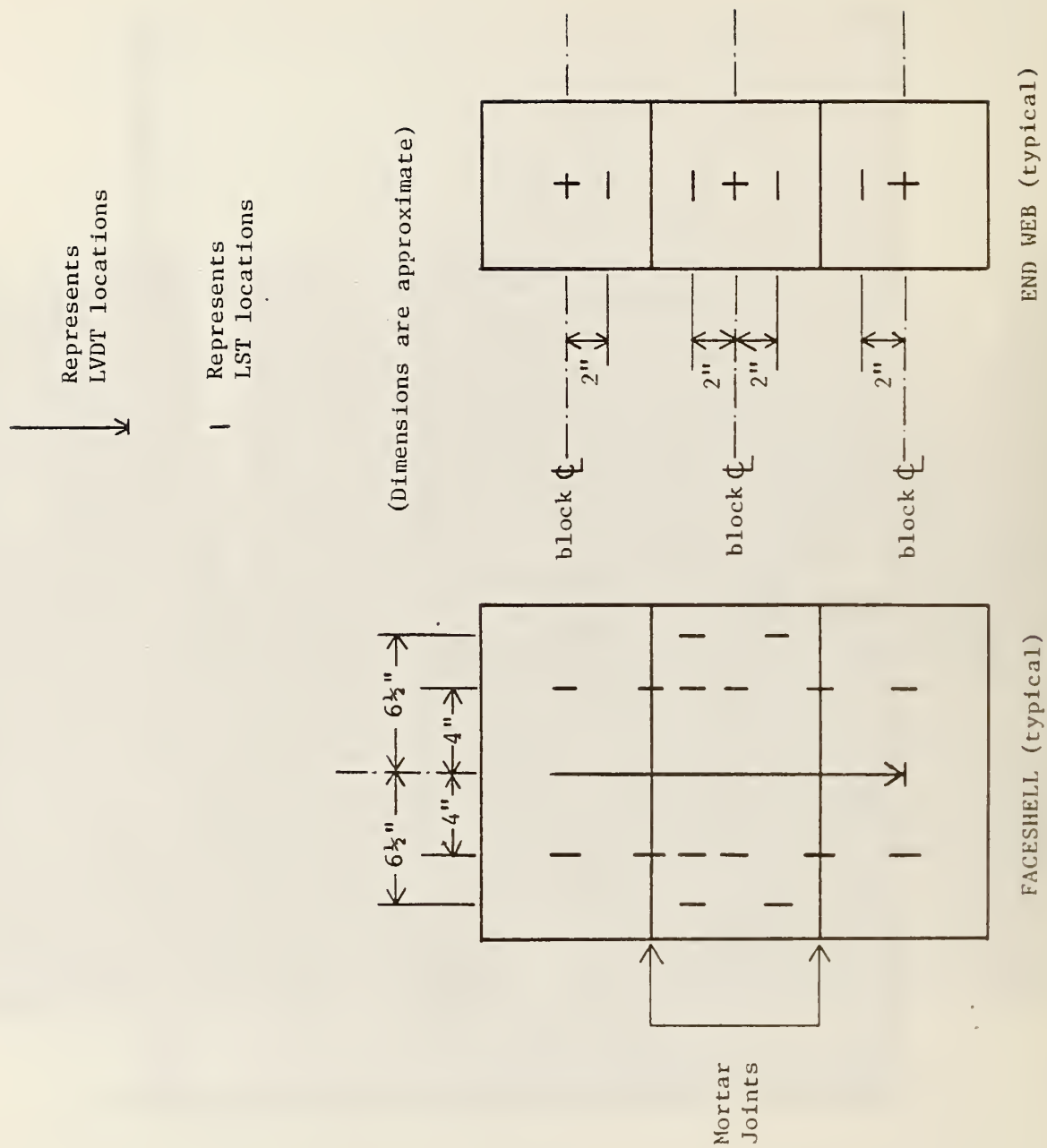


Figure 2.6 Locations of LST's and LVDT's

the same position on all of the prisms. Thus, comparisons among the various types of prisms were made using LVDT data. The short gage length of an LST rendered LST data sensitive to local effects. This had advantages and disadvantages. The principal advantage was that this made possible the measurement of strain distribution in a prism. The major disadvantage was that adverse local flaws such as voids could dramatically affect the measured data. In general, LST data was less consistent numerically than was LVDT data but was valuable in the identification of general trends.

3. MASONRY PRISM STRENGTH ANALYSIS

This section examines the influence of block strength, mortar strength, and mortar bedding configuration on masonry prism compressive strength. Also included in this section is a description of the modes of failure of the prisms. In all tables in this section, the following codes are used for simplicity:

HM = high-strength mortar	LM = low-strength mortar
HB = high-strength block	LB = low-strength block
FS = faceshell bedding	FB = full-area bedding

Masonry prism strengths were calculated in accordance with ASTM E447[1], i.e., as maximum load sustained divided by the net cross-sectional area of the prism. The computed compressive strengths and elastic moduli of prisms are listed in Tables 3.1 and 3.2 for faceshell-bedded prisms and full-area-bedded prisms. Moduli for these prisms were computed as the slope of the least-squares linear regression for stresses (based on net cross-sectional area of prisms) on strains (computed by dividing deformations measured by LVDT's by gage length) for stresses between zero and 0.33 f'_m. Also listed in Tables 3.1 and 3.2 are the average compressive strengths, the standard deviations of the strengths, and the coefficients of variation of strength for each group of prisms having the same block strength, mortar type, and configuration of mortar bedding.

3.1 MODES OF FAILURE

Failure was defined as the condition where the specimen under test could no longer sustain the applied load. Prisms cracked prior to reaching their failure loads. The crack patterns were indicative of the mode of failure of the specimen. Results from this study indicate that the mode of failure was strongly dependent on the type of mortar bedding used in the prism.

Prisms that were mortared on the net cross-sectional area (full-area bedding) exhibited compressive shear failures across one or more blocks of the prism. A typical failure is pictured in figure 3.1. Compressive shear failure was shown by diagonal cracking through the thickness of a faceshell or web of the prism element, such that the masonry bounded by cracks fell off. Partial splitting of the faceshells along a plane parallel to the faceshell was common in full-area-bedded prisms. This type of splitting was more common in faceshells than in webs of full-area-bedded prisms.

Table 3.1 Faceshell-Bedded Masonry Prism Compressive Strength

High-Strength Block
Net Cross-Sectional Area = 61.5 sq. in.

<u>Low-Strength Mortar</u>			<u>High-Strength Mortar</u>		
Prism Identifier	Strength (psi)	E_m (ksi)	Prism Identifier	Strength (psi)	E_m (ksi)
5-1-1	2159	1181	3-1-2	1911	1005
5-1-2	1992	820	3-1-3	1874	1017
5-1-3	1951	813	3-1-4	1675	1181
5-1-4	2094	1026	3-3-1	2093	973
5-4-1	1976	1080	3-3-2	2059	1079
5-4-2	1870	829	3-3-3	2133	1069
5-4-3	1894	1032	3-4-1	2146	1181
5-4-4	1951	1059	3-4-2	2187	1068
			3-4-3	2069	1057
			4-1-1	1930	1056
			4-1-2	2041	1037
			4-1-3	2179	1121
			4-3-1	1801	872
			4-3-2	2024	996
			4-3-3	1927	*
<hr/> Average Stress = 1986 psi			<hr/> Average Stress = 2003 psi		
Std. Deviation = 97 psi			Std. Deviation = 147 psi		
Coef. of Var. = 4.9%			Coef. of Var. = 7.4%		
			* Data not Available		

Low-Strength Block
Net Cross-Sectional Area = 60.4 sq. in.

<u>Low-Strength Mortar</u>			<u>High-Strength Mortar</u>		
Prism Identifier	Strength (psi)	E_m (ksi)	Prism Identifier	Strength (psi)	E_m (ksi)
6-7-1	1589	851	6-1-1	1598	959
6-7-2	1474	651	6-1-2	1672	990
6-7-3	1502	787	6-1-3	1623	964
6-9-1	1474	896	6-3-1	1474	510
6-9-2	1416	723	6-3-2	1556	952
			6-3-3	1536	960
			6-10-1	1395	1042
			6-10-3	1391	758
			6-12-1	1631	1036
			6-12-2	1507	669
			6-12-3	1477	907
<hr/> Average Stress = 1491 psi			<hr/> Average Stress = 1533 psi		
Std. Deviation = 63 psi			Std. Deviation = 94 psi		
Coef. of Var. = 4.2%			Coef. of Var. = 6.1%		

Table 3.2 Full-Area-Bedded Masonry Prism Compressive Strengths

High-Strength Block
Net Cross-Sectional Area = 61.5 sq. in.

<u>Low-Strength Mortar</u>		<u>High-Strength Mortar</u>	
Prism Identifier	Strength (psi)	Prism Identifier	Strength (psi)
No prisms of this type were tested.		3-2-1	2825
		3-2-2	2650
		3-2-3	2967
		3-5-1	2431
		3-5-2	2854
		3-5-3	2650
		3-6-1	2675
		3-6-2	2691
		3-6-3	2618
		4-2-1	2528
		4-2-2	2764
		4-2-3	2553
		4-4-1	2894
		4-4-2	2675
		4-4-3	2780
		Average Stress = 2704 psi	
		Std. Deviation = 145 psi	
		Coef. of Var. = 5.4%	
		* Data not Available	

Low-Strength Block
Net Cross-Sectional Area = 60.4 sq. in.

<u>Low-Strength Mortar</u>			<u>High-Strength Mortar</u>		
Prism Identifier	Strength (psi)	E_m (ksi)	Prism Identifier	Strength (psi)	E_m (ksi)
6-6-1	1999	1193	6-2-1	2045	1106
6-6-2	1954	1236	6-2-2	1921	990
6-6-3	1912	919	6-2-3	2136	1125
6-8-1	2078	1215	6-4-1	2119	1122
6-8-2	1921	978	6-4-2	2161	1184
6-8-3	1950	1196	6-4-3	2119	1250
			6-11-1	1995	1176
			6-11-2	2119	1215
			6-11-3	2169	1021
			6-13-1	2103	1322
			6-13-2	1958	1257
			6-13-3	2016	1332
Average Stress = 1969 psi			Average Stress = 2072 psi		
Std. Deviation = 62 psi			Std. Deviation = 82 psi		
Coef. of Var. = 3.1%			Coef. of Var. = 4.0%		

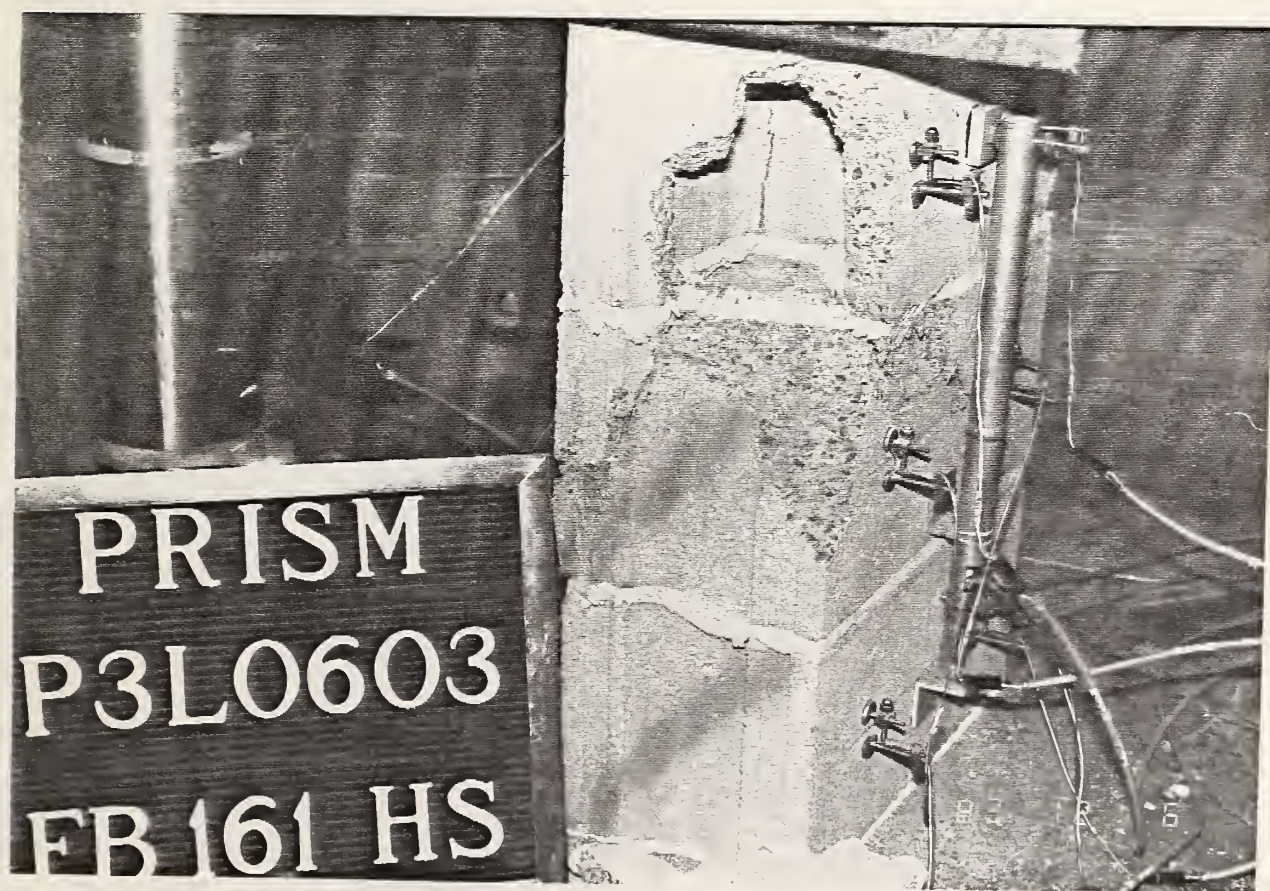


Figure 3.1 Failure of a full-area-bedded prism

Webs cracked along an essentially vertical line at about one-half (40 to 60 percent) of the failure load in prisms that were mortared on only the faceshells. As will be discussed later, web cracking was due to bending introduced by the web loading condition. This cracking occurred in the webs of the middle blocks of all prisms and in most of the webs of the top and bottom blocks of the faceshell-bedded prisms in this study. A typical faceshell-bedded prism at failure is pictured in figure 3.2. Once the web cracks formed, they extended rapidly with increasing load. Web cracking produced two columns consisting of faceshells, whose degree of interaction changed with increasing load. This configuration was apparently stable up to failure for three-unit-high prisms. The faceshells sometimes cracked through their thickness as described for full-area-bedded prisms.

3.2 EFFECT OF BEDDING TYPE

Bedding type had a significant effect on the average ultimate load capacity of the prisms tested as part of this study. Prisms constructed with faceshell bedding failed at lower applied loads than did prisms constructed with full-area bedding. For a single combination of block strength and mortar strength, the ratio of average ultimate load capacity of prisms constructed with faceshell bedding to that of prisms constructed with full-area bedding was about 0.75. A listing of this ratio for all mortar and block strength combinations is contained in Table 3.3. The uniformity of this ratio indicated that the influence of bedding type on strength was unaffected by the properties of the materials used to construct the prisms.

Table 3.4 contains the average prism compressive strengths for all prisms constructed with the same mortar strength, block strength and mortar bedding type for all combinations tested. The compressive strengths were based on net cross-sectional area. The data in Table 3.4 suggests that the ultimate stresses developed in faceshell-bedded prisms were less than the ultimate stresses developed in full-area-bedded prisms constructed from comparable materials. However, this apparent difference was due to the use of a common area to calculate stresses when, in fact, faceshell-bedded prisms had a different bearing area than did full-area-bedded prisms. Mortared area was the actual effective bearing area between blocks of a prism. Stresses calculated on the basis of mortar-bedded area can be expected to be similar for equivalent materials.

Bedding type had a significant effect on the amount of scatter of the values of ultimate strength of prisms constructed of comparable materials. The coefficient of variation of the ultimate stresses for the faceshell-bedded prisms was higher than for full-area-bedded prisms for all material strength combinations. Table 3.5 contains the coefficients of variation for all combinations of material strengths and bedding types.



Figure 3.2 Failure of a faceshell-bedded prism

Table 3.3 Ratio of Average Compressive Strengths
Faceshell to Full-Area Bedding

	<u>HM - HB</u>	<u>HM - LB</u>	<u>LM - HB</u>	<u>LM - LB</u>
Faceshell-Bedded	2003	1533	1986	1491 (psi)
Full-Area-Bedded	2704	2072	----	1969 (psi)
Ratio (FS / FB)	0.74	0.74	----	0.76

Table 3.4 Average Compressive Strengths by Group

<u>Prism Group Characteristics</u>	<u>Compressive Strength (psi)</u>
HM - HB - FS	2003
HM - HB - FB	2704
LM - HB - FS	1986
LM - HB - FB	----
HM - LB - FS	1533
HM - LB - FB	2072
LM - LB - FS	1491
LM - LB - FB	1969

It also appears that, as overall prism strength increased, the coefficient of variation of the strengths also increased. However, this trend may be due in part to the fact that fewer tests were conducted using prisms having lower strengths. For the typical number of tests, scatter of data could be expected to increase as sample size increased because of the variable nature of masonry prisms.

3.3 EFFECT OF MORTAR STRENGTH

The effect of variations in mortar strength on the ultimate load sustained by a prism was small. This observation was based on a comparison of the ultimate stresses achieved by prisms constructed with low-strength mortar to the ultimate stresses achieved by prisms made with high-strength mortar. The comparison was most conveniently made by comparing the ratios of ultimate stresses developed in prisms which were similar except for mortar strength. The values of the ratios of average compressive strengths for the different combinations were all nearly equal to one, as shown in Table 3.6. This fact suggests that the effect of mortar strength on masonry prism strength was negligible. Such a conclusion is reinforced by noting that the ratio of the average mortar compressive strengths for the two mortar types was 0.66. Clearly, if mortar strength had been a significant determinant of prism strength, the ratio of masonry prism strengths would not have been unity, but some value more nearly equal to 0.66. Thus, it is reasonable to state that variations in mortar strength had a negligible effect on a prism's compressive strength.

3.4 EFFECT OF BLOCK STRENGTH

The effect of block strength on overall prism strength can be determined by comparing average ultimate stress among prisms constructed with the same mortar type and mortar bedding, but with blocks of different strengths. This comparison was most easily made by using ratios of average compressive strength of prisms made with low-strength block to the average compressive strength of prisms made with high-strength block. The ratios, listed in Table 3.7, were all approximately 0.75, regardless of the combination of mortar type and mortar bedding. Thus, the effect of changes in block strength on prism strength was significant. The ratio of the unit compressive strength of the low-strength block to the compressive strength of the high-strength block was approximately 0.72. The strength ratio for the block approximated the strength ratio for the prisms. Not only was the effect of block strength on prism strength significant, but the effect seemed to be predicted by the simple ratio of block unit strengths. This result also demonstrated that block strength was significantly more influential than mortar strength in its effect on the load carrying capacity of a prism.

Table 3.5 Coefficient of Variation of Compressive Strengths

	<u>HM - HB</u>	<u>HM - LB</u>	<u>LM - HB</u>	<u>LM - LB</u>
Faceshell-Bedded	7.4%	6.1%	4.9%	4.2%
Full-Area-Bedded	5.4%	4.0%	-----	3.1%

Table 3.6 Ratio of Average Compressive Strengths
Low to High Strength Mortar

	<u>HB - FS</u>	<u>HB - FB</u>	<u>LB - FS</u>	<u>LB - FB</u>
Low-Str Mortar	1986	-----	1491	1969 (psi)
High-Str Mortar	2003	2704	1533	2072 (psi)
Ratio (LM / HM)	0.99	-----	0.97	0.95

Table 3.7 Ratio of Average Compressive Strengths
Low to High Strength Block

	<u>LM - FS</u>	<u>HM - FS</u>	<u>LM - FB</u>	<u>HM - FB</u>
Low-Str Block	1491	1533	1969	2072 (psi)
High-Str Block	1986	2003	-----	2704 (psi)
Ratio (LB / HB)	0.75	0.77	-----	0.77

4. PRISM STRAIN DISTRIBUTION

In this chapter, data are presented which describe the distribution of strain in the prisms. Strain measurements are reported which support the observed difference in behavior between faceshell-bedded and full-area-bedded prisms. Results of a simple, linear elastic finite element analysis are shown which graphically illustrate prism behavior. Measured strain data are presented which support the predicted behavior.

The strain data used in this chapter and elsewhere in this report are computed values taken as the displacement measured by an LST or LVDT divided by the appropriate gage length. The strain data are from LST's unless otherwise specified. The sign convention is that tensile strains are positive and compressive strains are negative.

4.1 UNIFORMITY OF STRAIN

This section describes the nature of the strain distributions in full-area-bedded and faceshell-bedded prisms. The measured strain distributions indicated that mortar bedding type significantly affected the uniformity of strain distribution and the strain magnitude within a prism.

4.1.1 Full-Area-Bedded Prisms

Strain in the webs of full-area-bedded prisms was uniform in magnitude over the web. Strain data indicated that the webs carried load predominantly by vertical compression: lateral tensile strains were small. The magnitude of lateral strains in webs was comparable among blocks, as was the magnitude of vertical strains in webs (figs. 4.1 and 4.2).

The strain data taken from faceshells of full-area-bedded prisms indicated that faceshell strains were uniform in distribution and in magnitude. Faceshells, like webs, resisted applied load predominately by vertical compression. In addition, the faceshell vertical strains were numerically similar to vertical web strains in material-equivalent prisms (fig. 4.3). Values of vertical strains were similar for all blocks of prisms having full-area bedding. A typical comparison of vertical strains in webs of the blocks at all levels of load may be found in figure 4.4. The strain history illustrated in the figure is regular and linear.

4.1.2 Faceshell-Bedded Prisms

Strains measured during tests of faceshell-bedded prisms varied significantly in magnitude and distribution within both webs and faceshells of prisms. The magnitudes of vertical strains in webs were different among vertically aligned webs of a prism as shown

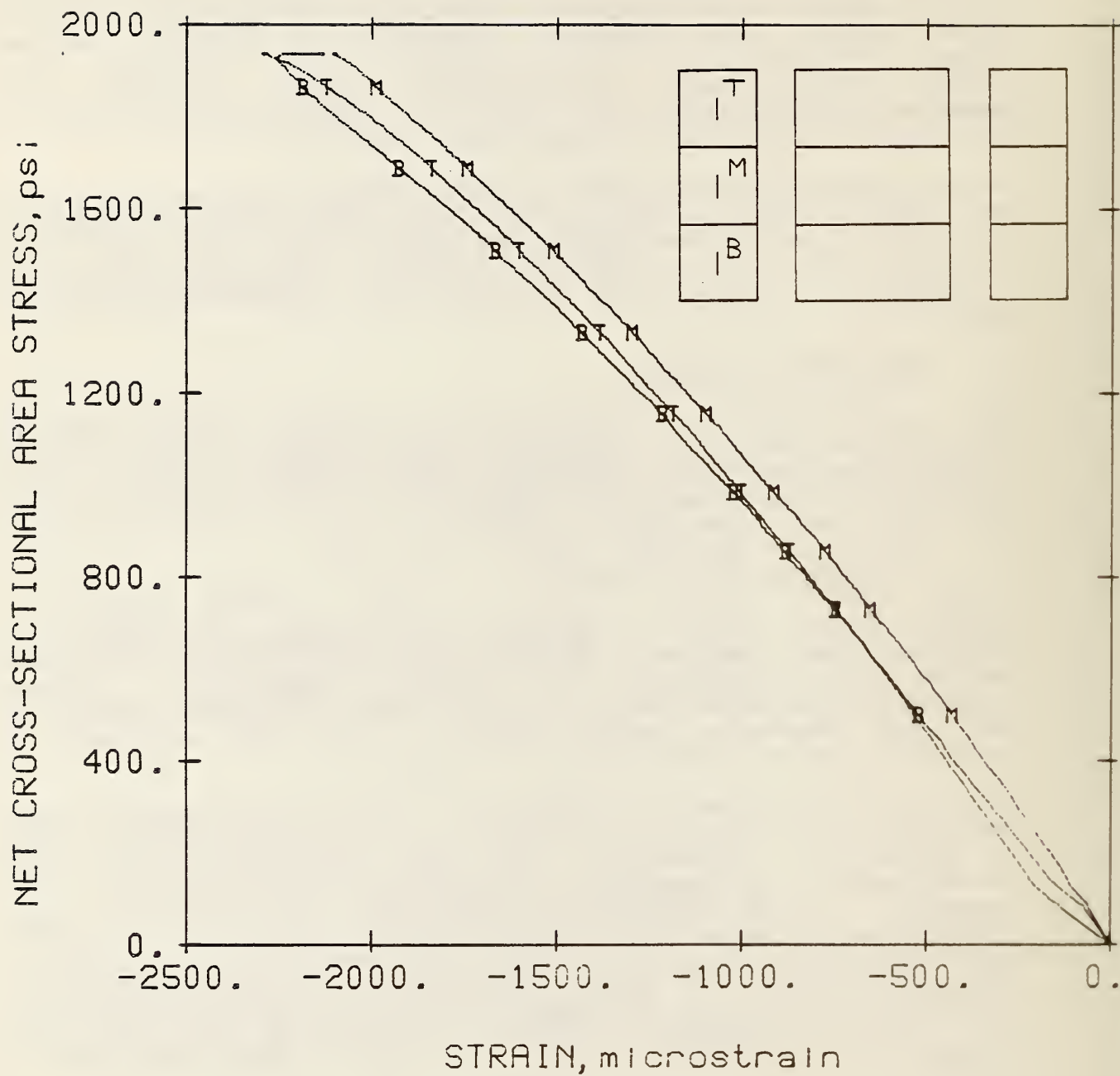


Figure 4.1 Web vertical strain by block for full-area-bedded prisms.

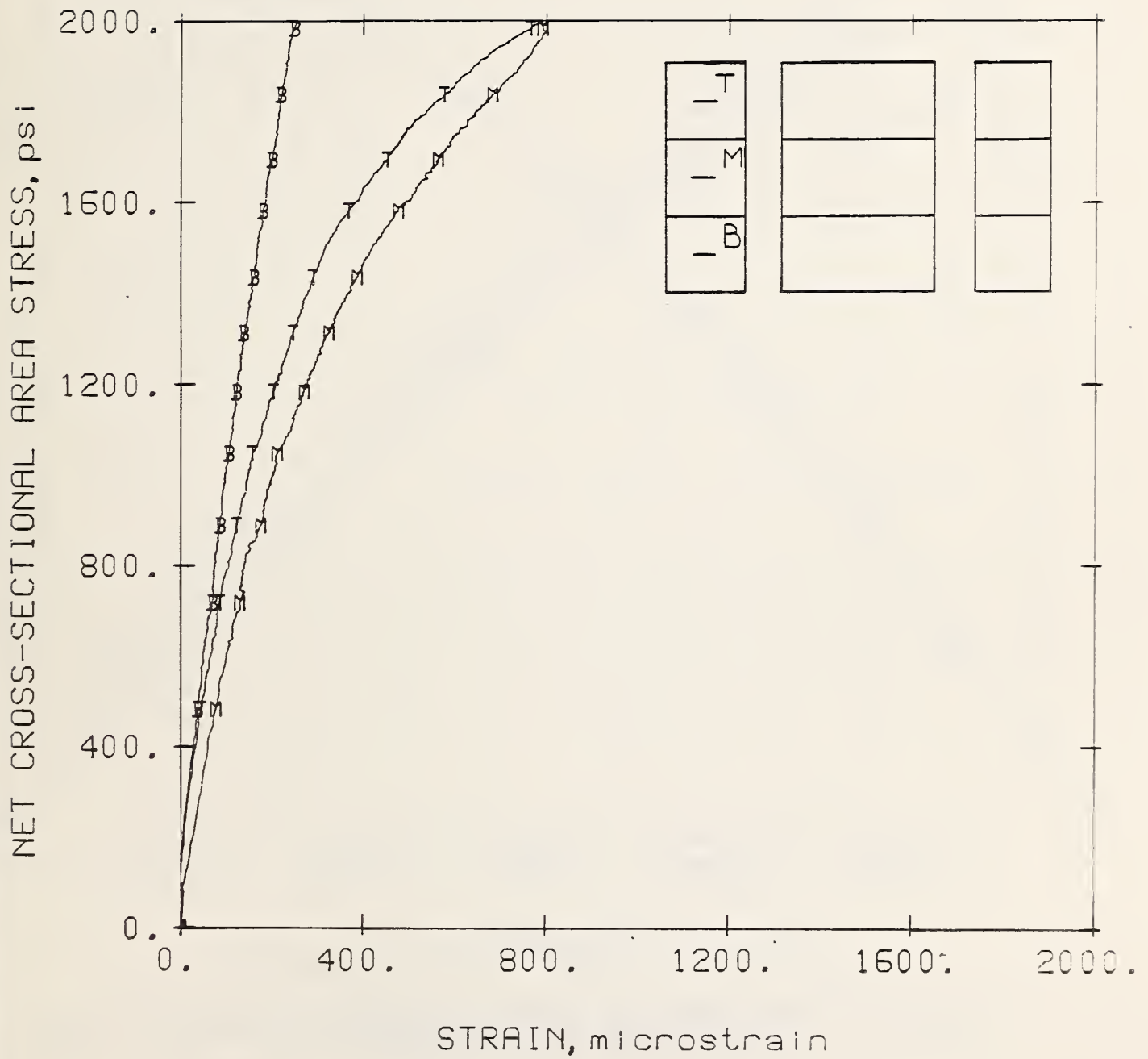


Figure 4.2 Web lateral strain by block for full-area bedded prisms.

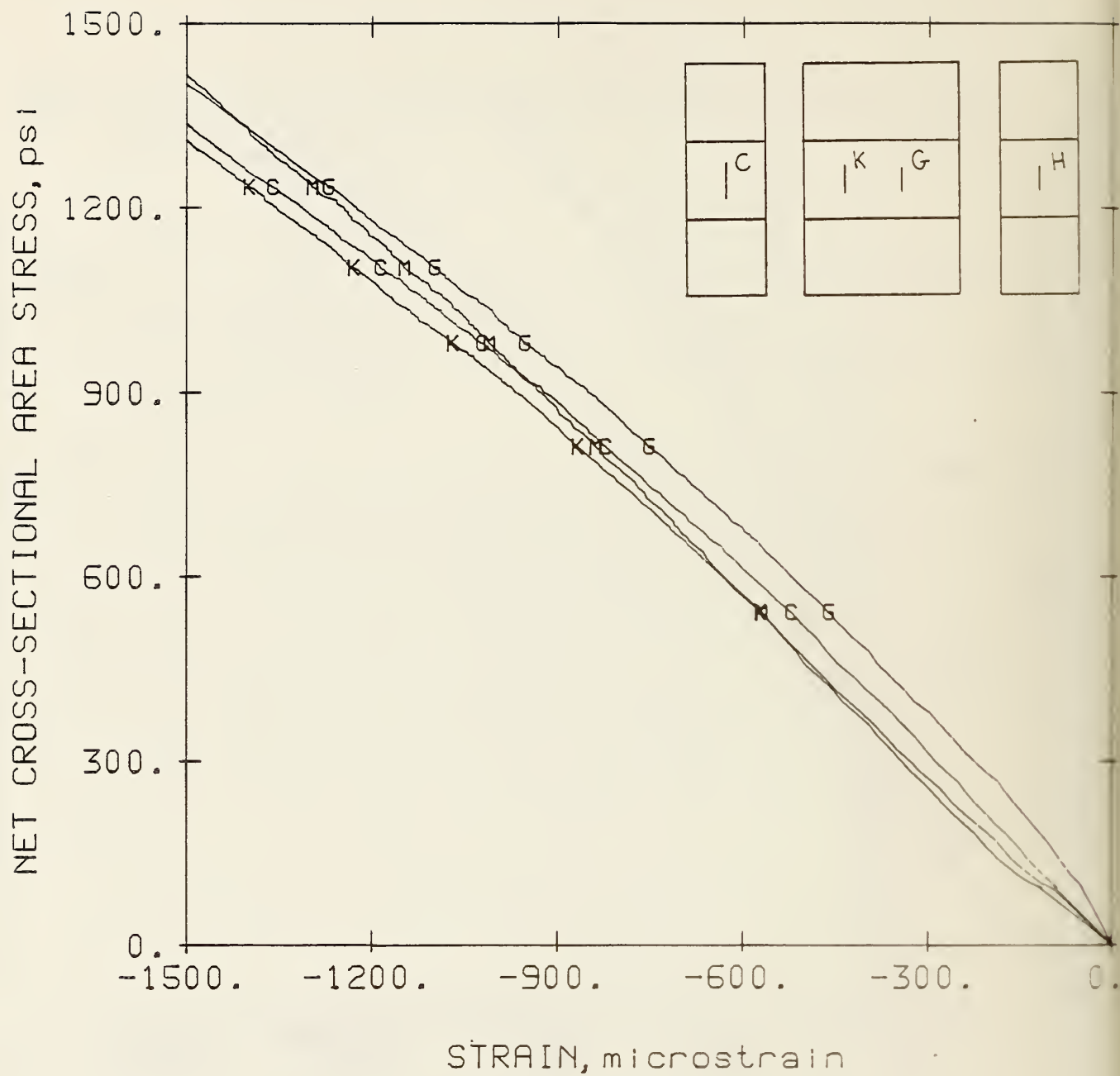


Figure 4.3 Comparison of vertical strains - faceshell to web for full-area-bedded prisms.

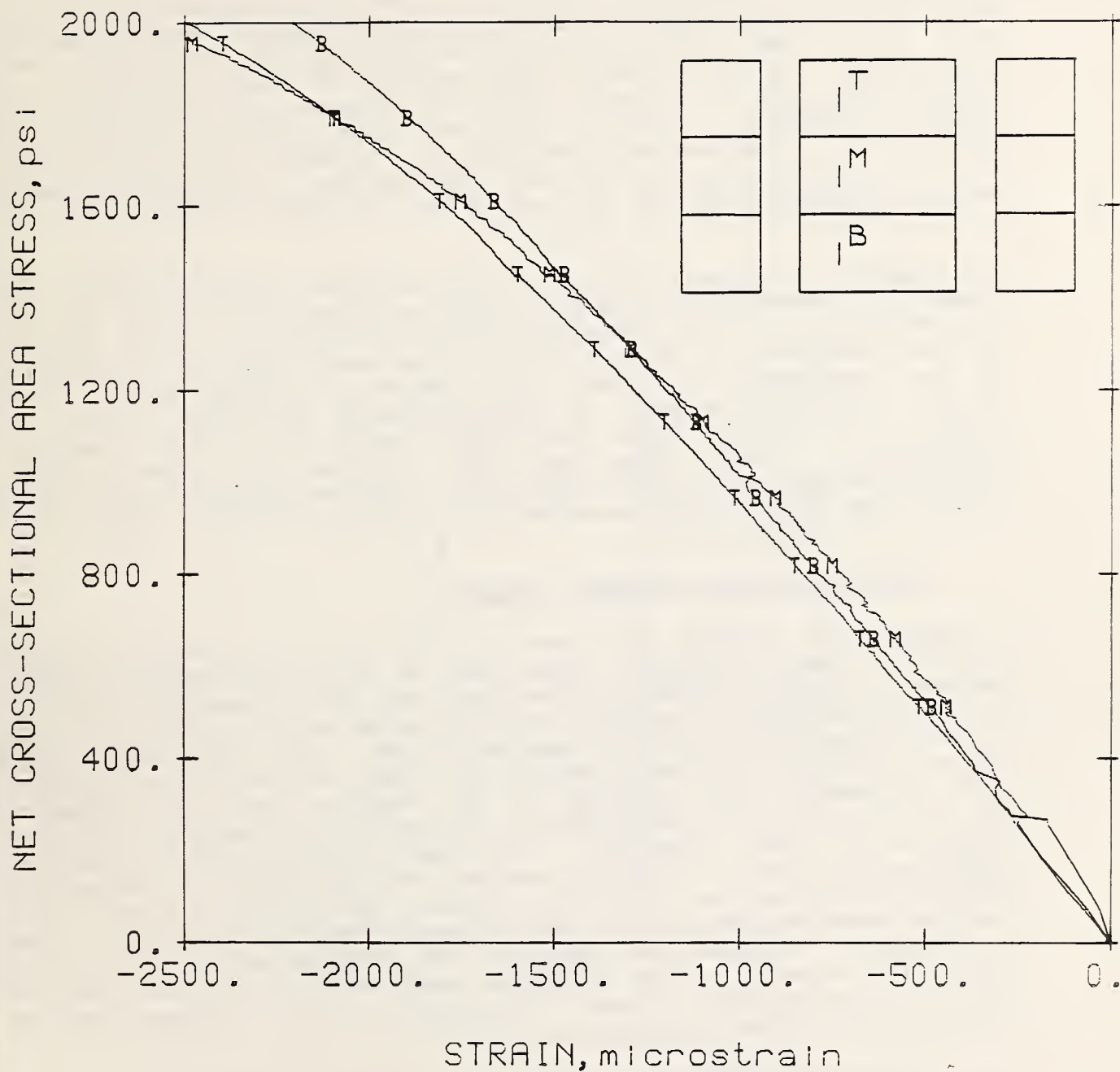


Figure 4.4 Comparison of faceshell vertical strain by block for full-area-bedded prisms.

in figure 4.5. Vertical strains in the webs of the middle block were smaller than vertical strains in the webs of the end blocks (fig. 4.6). The larger vertical strains in the end blocks were most likely due to the fact that the end bearing surfaces of the prisms were fully capped. While this was in accordance with typical practice, it caused the end block webs to be directly loaded by the testing machine platens. However, the middle block webs were not directly loaded because no mortar was present between the webs of the end and middle blocks of the faceshell-bedded prisms.

The webs of the middle block of the faceshell-bedded prisms were loaded by shearing forces transmitted from faceshells at the intersections of the webs and the faceshells. As a result, vertical compressive strains could have been expected to be large in the faceshells and small in the webs of the middle block relative to the strains in corresponding portions of the end blocks, which were more uniformly loaded in direct vertical compression. This behavior was verified in these tests. Measured strains in the faceshells of the middle block were larger than the strains measured in faceshells of the end blocks, as shown in figure 4.7.

4.2 MODE OF FAILURE AND WEB STRAINS

As previously stated, the mode of failure of faceshell-bedded prisms was very different from that of full-area-bedded prisms. The most distinguishable difference was the premature vertical web splitting which occurred at approximately 50 percent of the ultimate load for faceshell-bedded prisms. The full-area-bedded prisms typically did not crack until load was near the ultimate load. Clearly, the response to the applied load was different and, as a result, a significant difference in measured strains should have been observed. Measured differences in response supported the concept that premature web splitting in faceshell-bedded prisms was the result of bending induced in the web. Web bending occurred because of the support conditions at the prism bed joints. Because the response of webs appeared to be the aspect of behavior which differed most between faceshell-bedded and full-area-bedded prisms, this section will consider observed and predicted behavior of webs.

4.2.1 Faceshell-Bedded Prisms

The strain data acquired from the faceshell-bedded prisms indicated a strain distribution in the webs that was markedly different from that expected for a uniaxial compression test. Strain data were measured at too few locations to permit detailed mapping of the strain distribution. Thus, it was necessary to develop an analytical prediction of the strain distribution and confirm its validity with the strain data available. Finite element analysis techniques provided the analytical solution.

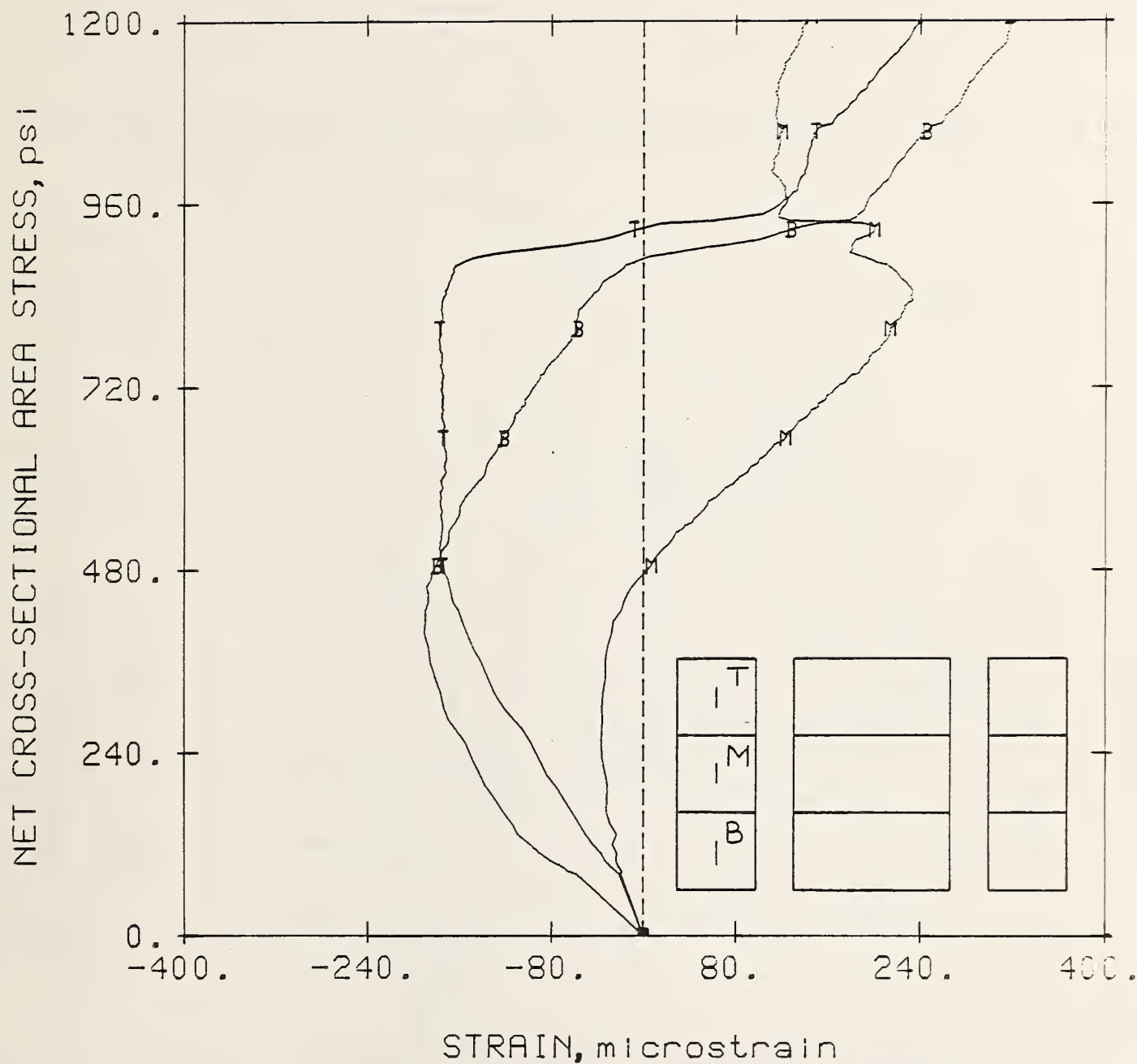


Figure 4.5 Comparison of web vertical strain by block for faceshell-bedded prisms.

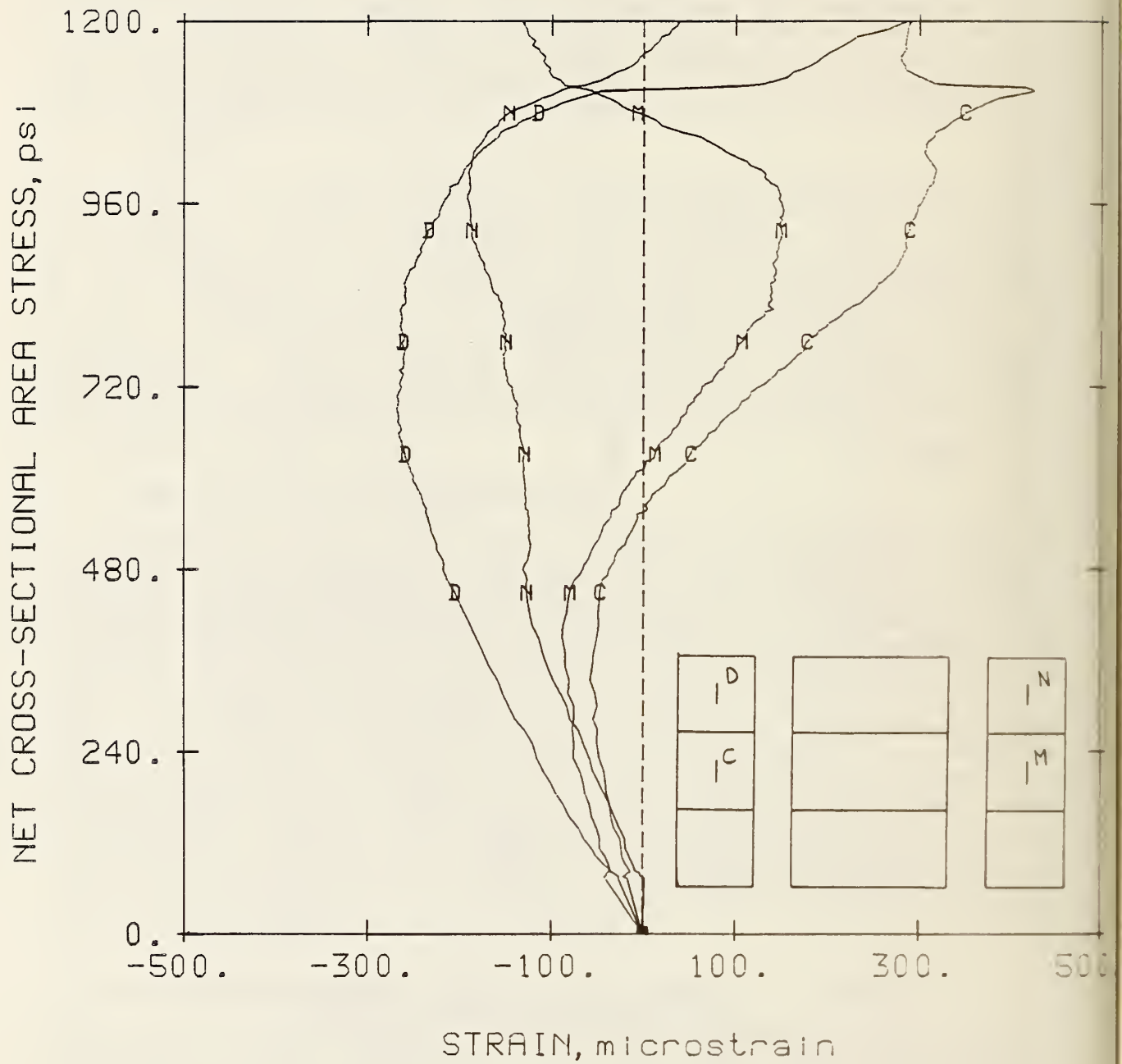


Figure 4.6 Influence of web stiffness on vertical strain distribution for faceshell-bedded prisms.

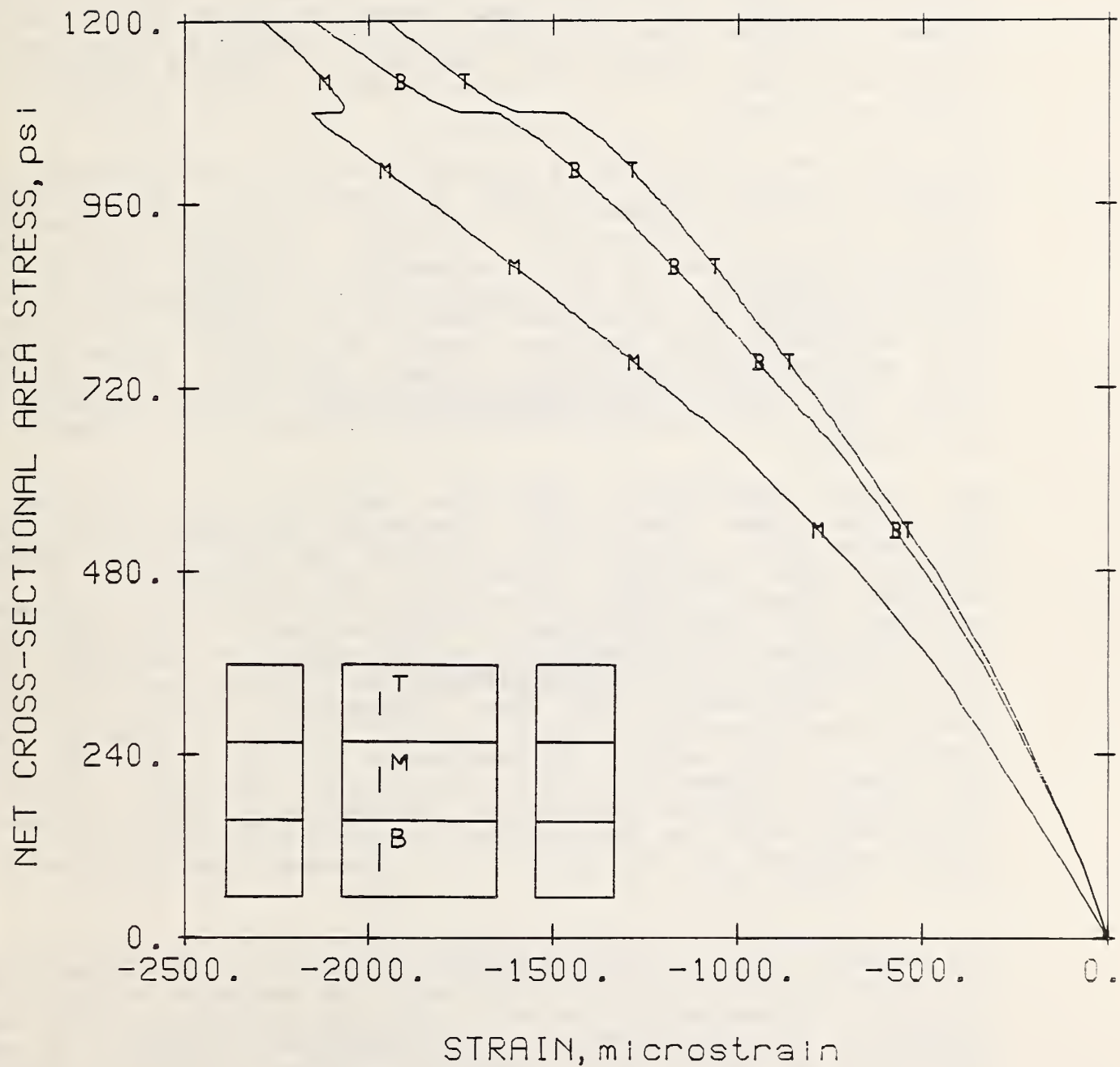


Figure 4.7 Comparison of faceshell vertical strains by block for faceshell-bedded prisms.

Details of the analysis may be found in Appendix A. Only the most pertinent results are noted in the subsequent discussions. The finite element analysis was useful as a predictor of stress (or strain) flow, but was not intended or used to quantitatively predict behavior. The graphical output of the analysis was in terms of stress flow, but because the analysis was linearly elastic and the results were compared to strains measured in uncracked prisms, a direct correspondence between stress and strain was assumed.

The predicted stress flow in a typical vertical line of webs in a faceshell-bedded prism is shown in figure 4.8. The deflected shape, although exaggerated for effect, indicates that bending takes place in all of the webs. As shown in figure 4.9, the webs could be considered to be an assemblage of beams, the top and bottom members of which had characteristics representative of a deep beam while the middle was something of a hybrid. The stress flow associated with deep beam action was similar to the stress flow predicted by the finite element analysis. Although the stress flow from the analysis was plausible, it was necessary to verify that the measured strain data qualitatively agreed with the analysis.

The first confirmation that the analysis had predicted a reasonable stress flow within a prism was provided by the fact that webs first cracked at locations at which high tension stresses were predicted (fig. 4.8). The distribution of the measured lateral strains in the web of the middle block also confirmed the appropriateness of the analysis. The predicted lateral stress/strain condition at the center of the middle web was compressive, which contradicted the expected behavior in a uniaxial compression test where compressive vertical strains should have produced tensile lateral strains. However, the measured lateral strain at the center of the middle web was consistently compressive until web cracking occurred. In fact, the measured lateral strains at the center of each web were compressive until the web cracked. Typical histories of lateral strain measured in the blocks of a faceshell-bedded prism are shown in figure 4.10.

Other confirmation of the predicted stress flow was provided by the measured vertical strains at the web centers. As illustrated in figure 4.6 for a typical prism test, the histories of vertical strain at the centers of the webs indicated compression until web cracking. More interestingly, the magnitude of strain in the middle web was much smaller than that in the end webs. Again, this was predicted by the analytical solution, which indicated a severely disturbed stress flow in the webs and vertical strains in the end webs larger than in the middle web. It was concluded that stress conditions in faceshell-bedded prisms were not comparable to the stress conditions assumed in uniaxial compression tests.

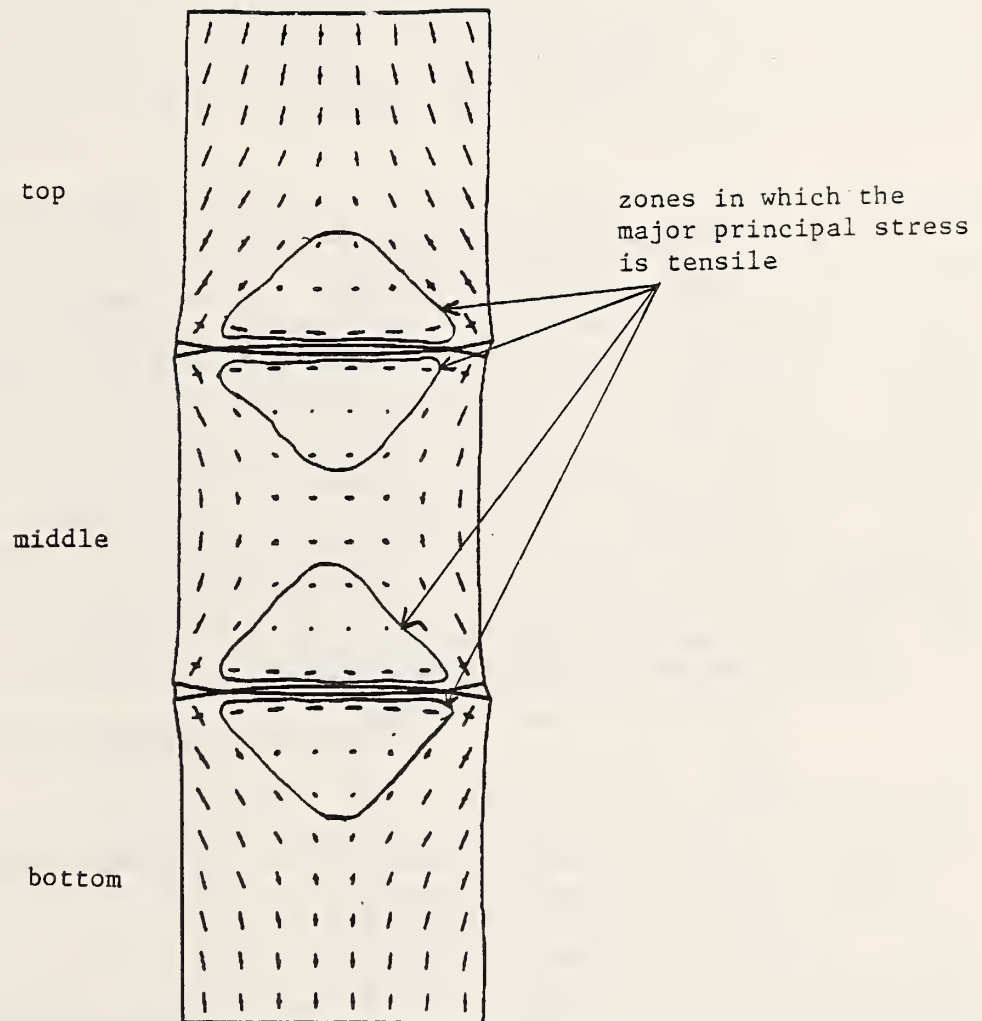


Figure 4.8 Stress trajectories in webs of a faceshell-bedded prism.

SUPPORT CONDITIONS

REACTION STRESSES

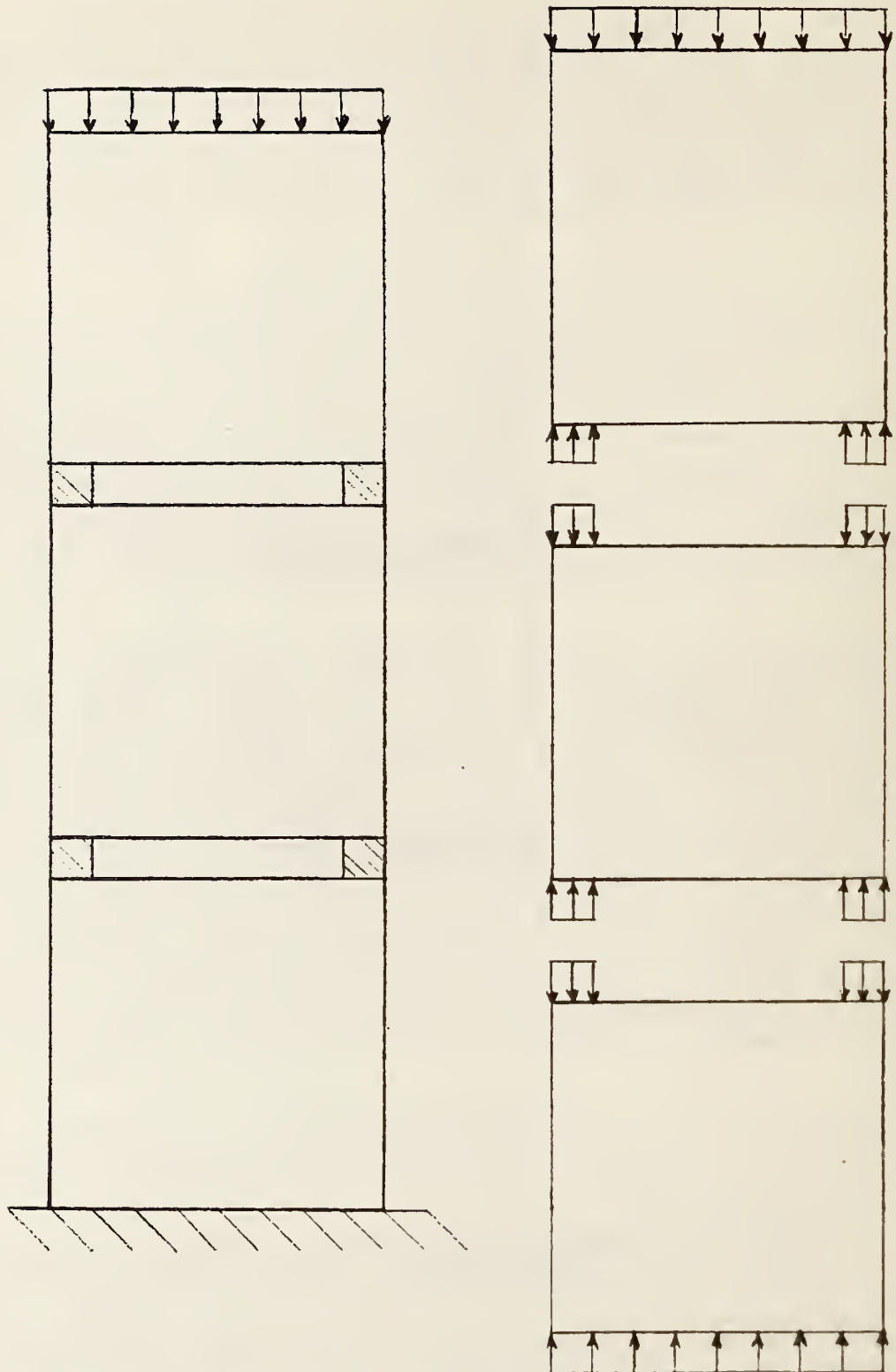


Figure 4.9 Support conditions for webs of faceshell-bedded prisms.

4.2.2 Full-Area-Bedded Prisms

Full-area-bedded prisms behaved much like prismatic members subjected to uniaxial compression. The measured strains in webs were consistently more uniform than those measured in webs of faceshell-bedded prisms. In addition, the vertical strains measured in the webs of full-area-bedded prisms were compressive, uniform and similar in magnitude to the vertical strains in faceshells. Small lateral tensile strains in webs resulted from unrestrained lateral expansion. To complement the analytical solution obtained for the faceshell-bedded prisms, the results of a similar finite element analysis for a full-area-bedded prism are presented.

The stress flow in the webs of a full-area-bedded prism predicted by the finite element analysis (figure 4.11) was very much as expected, with the stress flow being essentially undisturbed and the vertical stress being uniform. The measured web strains support the predicted stress flow by exhibiting essentially uniform vertical strain in all of the webs and small lateral tensile strains. The uniformity of vertical strain in a typical full-area-bedded prism is illustrated in figure 4.1, where histories of vertical strains measured in the end webs of all three blocks of a prism are shown. The lateral strains measured at the same locations are presented in figure 4.2. It is interesting to note that a typical ratio of lateral strain to vertical strain is approximately 0.15, which is a reasonable value for the poisson's ratio of concrete masonry. Clearly, the distribution of strains in full-area-bedded prisms was much more uniform and predictable than that in faceshell-bedded prisms.

4.2.3 Influence of Mortar Bedding

It has been demonstrated that reasonable predictions of stress/strain flow prior to prism cracking have been obtained for faceshell-bedded and full-area-bedded prisms. These stress flows suggested that webs split in faceshell-bedded prisms because of induced bending. In a brittle material such as concrete, whose capacity in tension is low, stress conditions which induce tensile stresses or strains are not desirable in a compression test. The bending introduced in the webs of faceshell-bedded prisms produced these unwanted tensile stresses. The finite element solution indicated that bending magnified tension stresses by at least three times over the stresses that would have resulted from the poisson effect alone in the zone of high tension stresses in the webs.

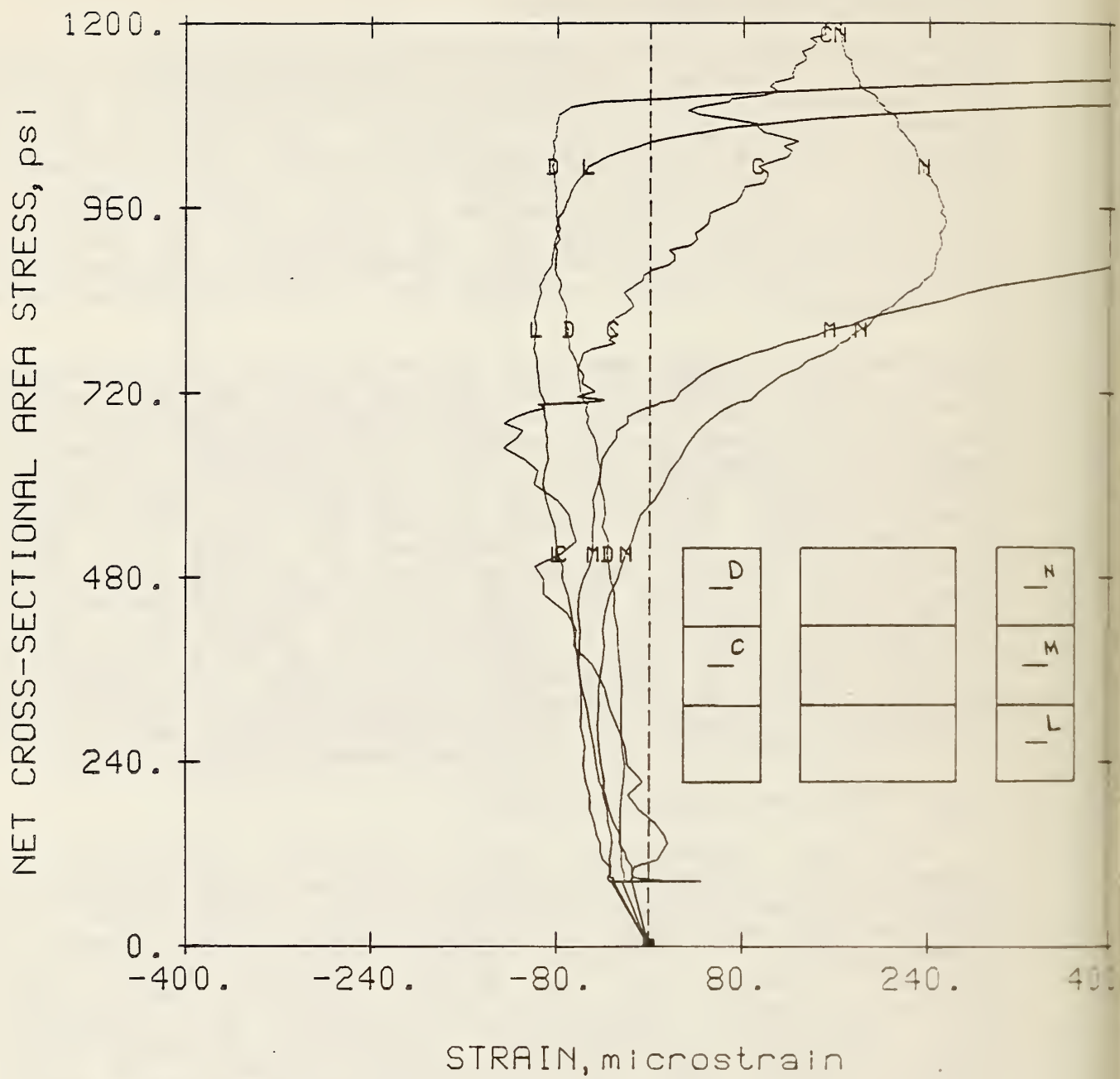


Figure 4.10 Web lateral strains by block for faceshell-bedded prisms.

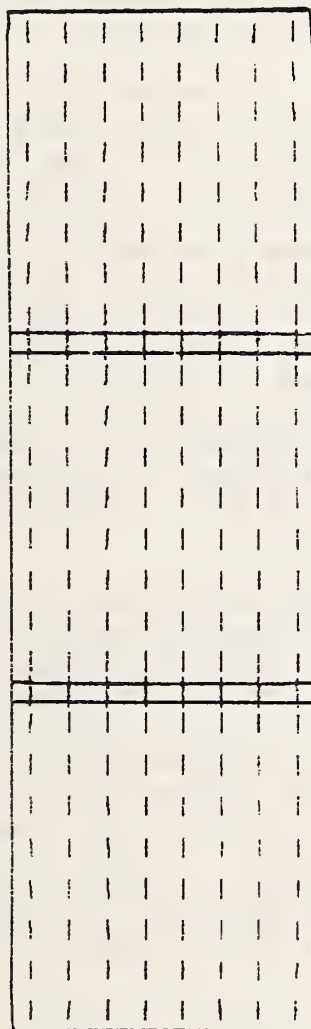


Figure 4.11 Stress trajectories in webs of a full-area-bedded prism.

4.3 STRAIN REDISTRIBUTION DUE TO WEB SPLITTING

As described in the previous section, webs in faceshell-bedded prisms split as a result of bending at approximately 50 percent of the prism's eventual ultimate load. As noted in Section 3.2, the ultimate load sustained by faceshell-bedded prisms was markedly lower than the ultimate load sustained by full-area-bedded prisms. It may be argued that the premature web cracking did eventually lead to early failure because the strain distribution in the prism changed when the webs split.

The strains measured in faceshell-bedded prisms indicated that strain redistribution in the prism began at the onset of web cracking and continued until failure. The redistribution of strain in faceshell-bedded prisms is illustrated by typical measured strain histories shown in figures 4.7 and 4.12. In figure 4.12, representative vertical faceshell strain histories are shown together with lateral web strains. The histories are all for the same prism. At the onset of web splitting, as the web strains abruptly became tensile, the faceshell vertical strains also changed abruptly. The change occurred with essentially no change in applied load, suggesting sudden strain redistribution. The change in vertical strain was of a different sense for the two histories. This change in sense of the strains was more important because it supported the previously described analytical solution.

The history of vertical strains in faceshells of all three blocks of a typical faceshell-bedded prism is shown in figure 4.7. The strains were measured along a vertical line on the prism and at the center of each block. The vertical strain in the middle block was consistently larger than the vertical strains in the end blocks prior to web cracking (strain shift). This was expected, as the web of the middle block supported very little of the applied load in direct vertical compression. Thus, the faceshells of the middle block carried more load than the faceshells of end blocks. When the webs split, the amount of load supported by the webs in the end blocks decreased and the amount of load supported by the faceshells in the end blocks increased.

The sudden decrease in compressive strain measured in the faceshells of the middle block was difficult to explain. The analytical solution suggested that the decrease resulted from a change in the amount of bending imposed on the middle block by the end blocks. The uncracked webs in the end blocks induced concave bending in the faceshells of the middle block. When the webs split, their ability to induce bending was diminished. Bending in faceshells of the middle block decreased, resulting in a decrease in the measured compressive strain.

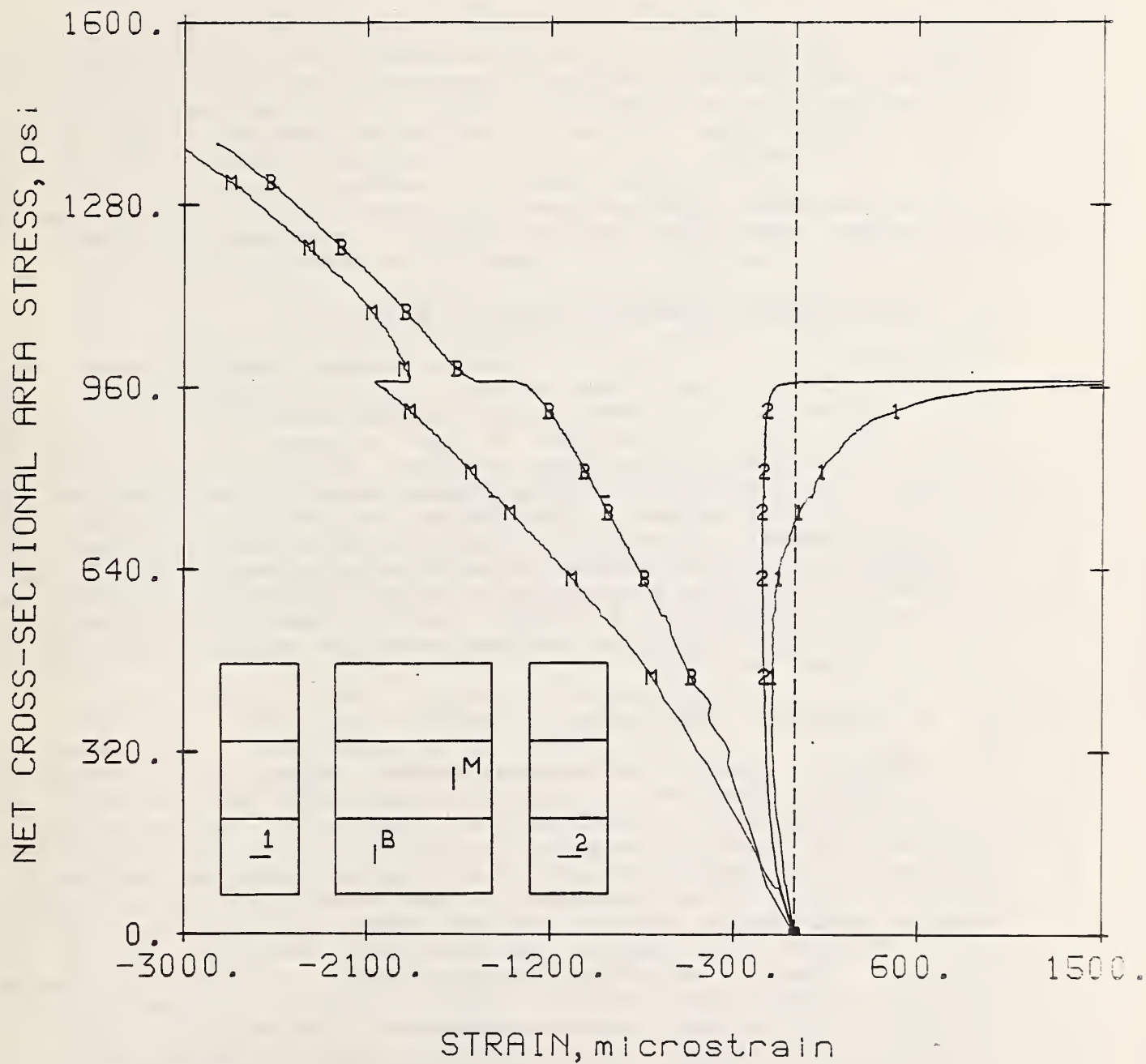


Figure 4.12 Strain redistribution after web cracking in faceshell-bedded prisms.

5. IMPLICATIONS OF RESULTS

The data presented in Chapters 3 and 4 demonstrate that mortar bedding configuration has a pronounced effect on prism behavior. Mortar bedding configuration affected prism compressive strength, the variability of strength, mode of failure, strain (stress) distribution, and strain distribution variability. The effects are interdependent and not easily isolated. The obvious differences in observed behavior between faceshell-bedded and full-area-bedded prisms suggest that the use of faceshell-bedded prisms to determine uniaxial masonry compressive strength is questionable, especially for quality control purposes.

5.1 COMPRESSIVE STRENGTH AND ITS VARIABILITY

The measured load capacities of the faceshell-bedded prisms were uniformly lower than those of the full-area-bedded prisms. For all combinations of materials, faceshell-bedded prisms could carry only about 72 percent of the ultimate load carried by full-area-bedded prisms. In addition, the variability of the strengths of faceshell-bedded prisms was larger than that of full-area-bedded prisms. The larger variability suggests that faceshell-bedded prisms are a less-suitable test specimen than are full-area-bedded prisms for obtaining a statistical measure of masonry compressive strength. The difference in ultimate load may be attributable to a reduced bearing area (faceshell mortar joint) or to the severely cracked condition of the prism due to premature web splitting.

5.1.1 Compressive Strength

In computing masonry prism compressive strength for a hollow block prism, the net cross-sectional area of the unit is typically used as the effective area. This area is easily obtained and normally reported as part of the unit properties. The use of the net cross-sectional area as the effective area is reasonable for full-area-bedded prisms because the mortar bedding area is nearly the same as the net cross-sectional area of the unit. However, the use of the net cross-sectional area of the unit is clearly not directly applicable to faceshell-bedded prisms. The effective area of such a prism is the area of mortar bedding, which is much less than the net cross-sectional area. However, the practicality of using the area of mortar bedding in computation of stress is questionable. The determination of actual mortar bedded area is tedious and would significantly increase the cost of conducting prism tests. An alternative to using the actual mortar bedded area is to assume an effective area that can be quickly calculated and is a realistic approximation of the faceshell-bedded prism's effective area. One possibility is to use the minimum faceshell area of the unit, i.e., the minimum faceshell thickness multiplied by twice the length of the faceshell. The faceshell thickness and length are

normally reported as unit properties. The use of faceshell area in calculating prism strength for faceshell-bedded prisms does not result in convergence between the compressive strengths reported for all prisms. The lack of comparability is evident in the values listed in Table 5.1. In this table, the average prism strengths have been computed on the basis of faceshell area for faceshell-bedded prisms and net cross-sectional area for full-area-bedded prisms.

In summary, the selection of an appropriate area to use when computing masonry compressive strength for faceshell-bedded prisms is somewhat arbitrary. In addition, while it may be possible to select an effective area for a faceshell-bedded prism which produces computed masonry strengths equal in magnitude to those obtained from full-area-bedded prisms, the variability of the data will not be decreased.

5.1.2 Variability of Compressive Strength

Prisms are used to obtain a measure of the uniaxial compressive strength of a masonry assemblage. The variability of the data from prism tests is an indicator of the confidence to be placed in the data. As the variability of data increases, the confidence we may have in the measured strengths decreases. As a result, lower values of masonry strength must be assumed for design purposes. It is desirable, therefore, to use a test procedure which minimizes the variability of the data.

On this basis alone, faceshell-bedded prisms are less desirable than are full-area-bedded prisms for determining masonry strength. Estimates of masonry compressive strength based on tests of faceshell-bedded prisms show large variability. It is inconsistent with the intent of a standard test to measure compressive strength using a test that permits alternate procedures for conducting the test, particularly when those alternate procedures result in different variabilities of measured strengths. Such a "standard" test, in which variability of estimated strength is not uniform, may be difficult to incorporate into masonry codes based on probabilistic design procedures that assume uniform factors of safety. However, even if the higher variability of measured masonry strengths inherent in the use of faceshell-bedded prisms is taken into consideration, the fact that failure modes of such prisms are not consistent with uniaxial compression can not be overlooked. A strain distribution other than that assumed and web splitting prior to prism failure make questionable the validity of tests using faceshell-bedded prisms to measure masonry compressive strength.

Table 5.1 Average Compressive Strength Based on Mortared Area

<u>CONSTRUCTION</u>	<u>STRENGTH (psi)</u>
HM HB FS	3107
HM HB FB	2690
LM HB FS	3072
LM HB FB	N/A
HM LB FS	2299
HM LB FB	2072
LM LB FS	2236
LM LB FB	1969

5.2 STRAIN DISTRIBUTION

Measured and analytically predicted strains indicated that full-area-bedded prisms behaved as uniaxially-compressed, prismatic members. The predominant strain (stress) was vertical, compressive, and relatively uniform through both cross-section and height. Cracking and/or spalling occurred at a load only slightly less than that at failure and the failure was typically sudden. It is reasonable to conclude that the maximum load carried by the prism divided by the solid cross-sectional area of the prism was a representative and consistent measure of the compressive strength of the masonry assemblage.

In sharp contrast to the strain distribution exhibited by full-area-bedded prisms, the strain distribution exhibited by faceshell-bedded prisms was strongly influenced by bending. The magnitudes of vertical strains in faceshells varied markedly along the prism height. The distribution of strains changed during a test due to premature web splitting resulting from the effects of bending. The web splitting divided the previously whole prism into two interacting columns whose principal vertical load resistance was provided by the faceshells. The effective bearing area changed during the test, making selection of an appropriate area for use in stress calculations difficult. The fact that the distribution of strains changed dramatically when the faceshell-bedded prisms split raises questions as to what is actually being measured when a faceshell-bedded prism fails. Because the distribution of strain changes as load is increased, it is not realistic to say that it is uniaxial compressive strength that is actually measured.

5.3 RECOMMENDATION

The data obtained from uniaxial compression tests of faceshell-bedded prisms indicated that such prisms should not be used to determine the compressive strength of masonry. Although the strengths of these prisms may adequately approximate the uniaxial compressive strength of faceshell-bedded walls, tests of faceshell-bedded prisms do not permit the calculation of a meaningful compressive strength. Because typical masonry design codes use masonry prism compressive strength as the basis for the determination of the strength of the masonry under other actions, such as shear, it is imperative that the measured masonry prism compressive strength be a well defined, repeatable quantity.

The data for faceshell-bedded prisms demonstrates that the load-carrying capacity of such prisms is strongly dependent on conditions which are not representative of uniaxial compression. Faceshell-bedded prisms exhibit strain distributions inconsistent with uniaxial compression. The compressive strength of faceshell-bedded prisms is more variable than that of prisms with full-area bedding and the effective bearing area of a faceshell-

bedded prism is difficult to determine. Both of these factors argue against the use of prisms with faceshell bedding as a standard of comparison.

It is suggested that only full-area-bedded prisms be used for determination of masonry compressive strength, regardless of the configuration of mortar bedding used in the actual masonry member the prisms are intended to represent. Such prisms have test conditions which can be more precisely controlled, have distributions of strain which are closer to an assumed condition of uniform strain, and have lower variability of strength than do faceshell-bedded prisms. The adoption of such a procedure will provide a material test method better suited to quality control applications than is the current procedure. As masonry design codes begin to be based on probabilistic estimates of material strength, they can use as their basic strength a single, well-defined compressive strength. It is recognized that the adoption of a single test procedure requires reformulation of design procedures to account for the new basis strength and the adoption of rational effective areas to be used in computing specific element stresses. However, these actions are best left to voluntary design standards development groups and are outside the scope of this report.

6. SUMMARY AND CONCLUSIONS

6.1 SUMMARY

Experimental data were presented from compression tests of seventy hollow, ungrouted, three-unit-high masonry prisms. The data included both load and deflection (strain) data and ultimate strengths. Block strength, mortar strength and mortar bedding configuration were varied. Block strength strongly influenced ultimate strength, but mortar strength did not. Mortar bedding configuration significantly affected the magnitude and variability of masonry prism compressive strength, strain distribution in prisms under uniaxial compression, and mode of failure of prisms. Analytical evaluations of strains in prisms supported the observed and measured behavior of prisms in the elastic range. The recommendation was made that only full-area-bedded prisms be used as quality control test specimens regardless of the mortar bedding configuration used in the masonry structure.

6.2 CONCLUSIONS

Several conclusions can be drawn on the basis of the strain and ultimate load data for the prisms.

- * The strain distributions in three-unit-high, hollow concrete masonry prisms are significantly affected by the configuration of mortar bedding.
- * The strain distributions in prisms under uniaxial compression are unaffected by changes in the strength of the materials used to construct the prisms.
- * Full-area-bedded prisms exhibit uniform stress-strain behavior that indicates uniaxial compression in all portions of a prism.
- * Faceshell-bedded prisms exhibit erratic stress-strain behavior that indicates compression in faceshells and bending in webs.
- * Faceshell-bedded prisms have ultimate loads which are lower than ultimate loads of full-area-bedded prisms.
- * Compressive strengths measured for faceshell-bedded prisms are less repeatable than are strengths measured for full-area-bedded prisms.

7. ACKNOWLEDGMENTS

The National Concrete Masonry Association provided the concrete block and the mason to fabricate the prisms. Mr. Frank Rankin prepared the prisms for testing and carried out the tests. Mr. Mark Hogan provided assistance in many ways during this project. Mr. Stuart Foltz assisted in preparation of the final report.

8. REFERENCES

1. "Compressive Strength of Masonry Prisms," (ASTM C447-74), ASTM Specifications for Concrete Masonry Units, American Society for Testing and Materials, Philadelphia, PA, pp. 29-32.
2. "Allowable Stresses," Building Code Requirements for Concrete Masonry Structures (ACI 531-79), American Concrete Institute, Detroit, MI, p. 30.
3. "Mortar for Unit Masonry," (ASTM C270-82), 1983 Annual Book of ASTM Standards, Vol. 4.01, American Society for Testing and Materials, Philadelphia, PA, pp. 250-254.
4. "Sampling and Testing Concrete Masonry Units," (ASTM C140-75), 1983 Annual Book of ASTM Standards, Vol. 4.05, American Society for Testing and Materials, Philadelphia, PA, pp. 117-120.

APPENDIX A. FINITE ELEMENT MODEL

A.1 MODEL

A simple finite element model was developed to aid in interpreting the experimental strain data. The results of this model were used as a predictor of trends in the strain data, but not as a numerical predictor of stress and/or strain. A commercial computer program having planar finite elements was used to model and analyze the prisms. Although results of the analyses were expressed in terms of stress, which could be graphically displayed, because the program was based on linear elastic behavior, the resulting stress flows were taken as direct representations of strain distribution.

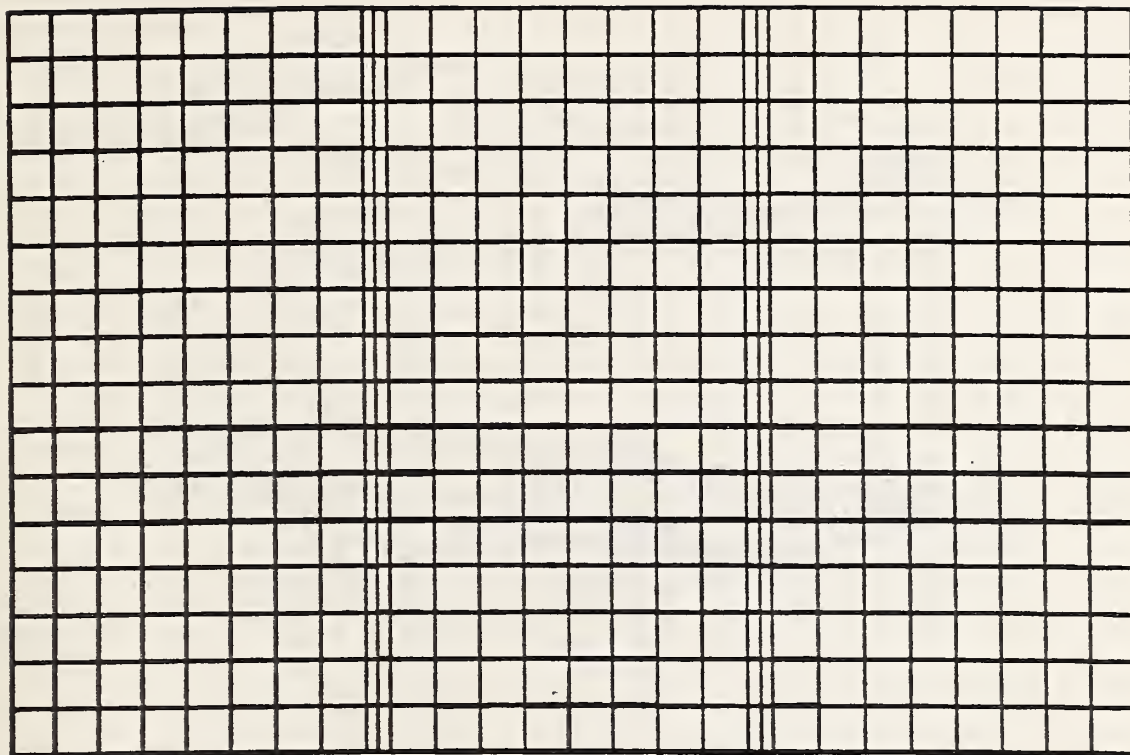
The prism was modeled as a three-dimensional assemblage of two-dimensional plate (membrane) elements. The analytical model of the prism was composed of five planes which represented the two faceshells and three webs. The faceshell plates were orthogonal to the web plates. Since the plates were discretized into membrane elements (fig. A.1), only stresses in the plane of the plate were computed. While the vertical stresses from all of the elements were parallel, the lateral (horizontal) stresses in the faceshells were oriented orthogonal to the lateral stresses in the webs. Thus, lateral stresses assumed the directions of their corresponding plates.

Principal stresses and their directions were also calculated. The term "major principal stress" described the maximum normal stress in an element and the term "minor principal stress" described the minimum normal stress in an element. The dimensions of the prism elements were taken as centerline dimensions (fig. A.2). The taper of the walls of the masonry unit along its height was disregarded. It was assumed that friction between the platens and the prism was sufficient to prevent any lateral expansion at those interfaces. Thus, lateral displacements were suppressed at the top and bottom end surfaces of the model prism. A uniform vertical applied stress equal to 1.0 psi was applied to the top surface of the model prism as illustrated in figure A.3. The vertical translation of the lower surface was suppressed to simulate lower platen support.

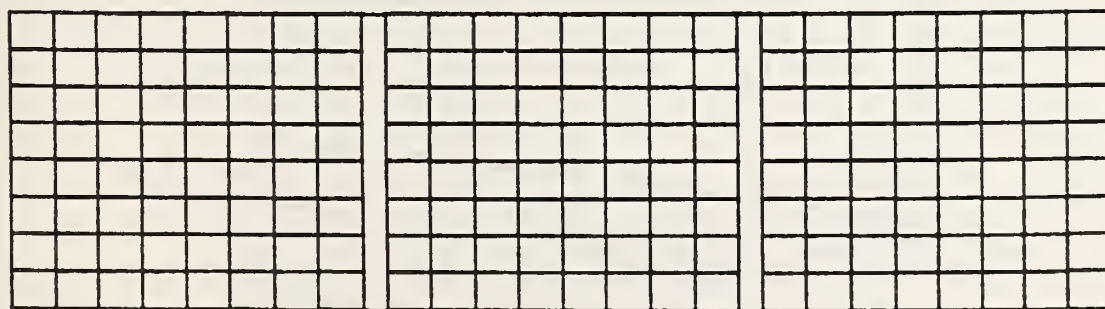
A.2 ANALYSIS

A.2.1 Full-Area-Bedded Prisms

According to the finite element analysis, webs of full-area-bedded prisms exhibit stresses typical of an element in uniaxial compression. The major principal stress orientation corresponds to the direction of loading in all webs of a prism. That is, stresses are largest in the vertical direction and are compressive (fig. 4.11). The magnitude of vertical stresses



typical faceshell mesh



typical web mesh

top block

middle block

bottom block

Figure A.1 Finite element mesh.

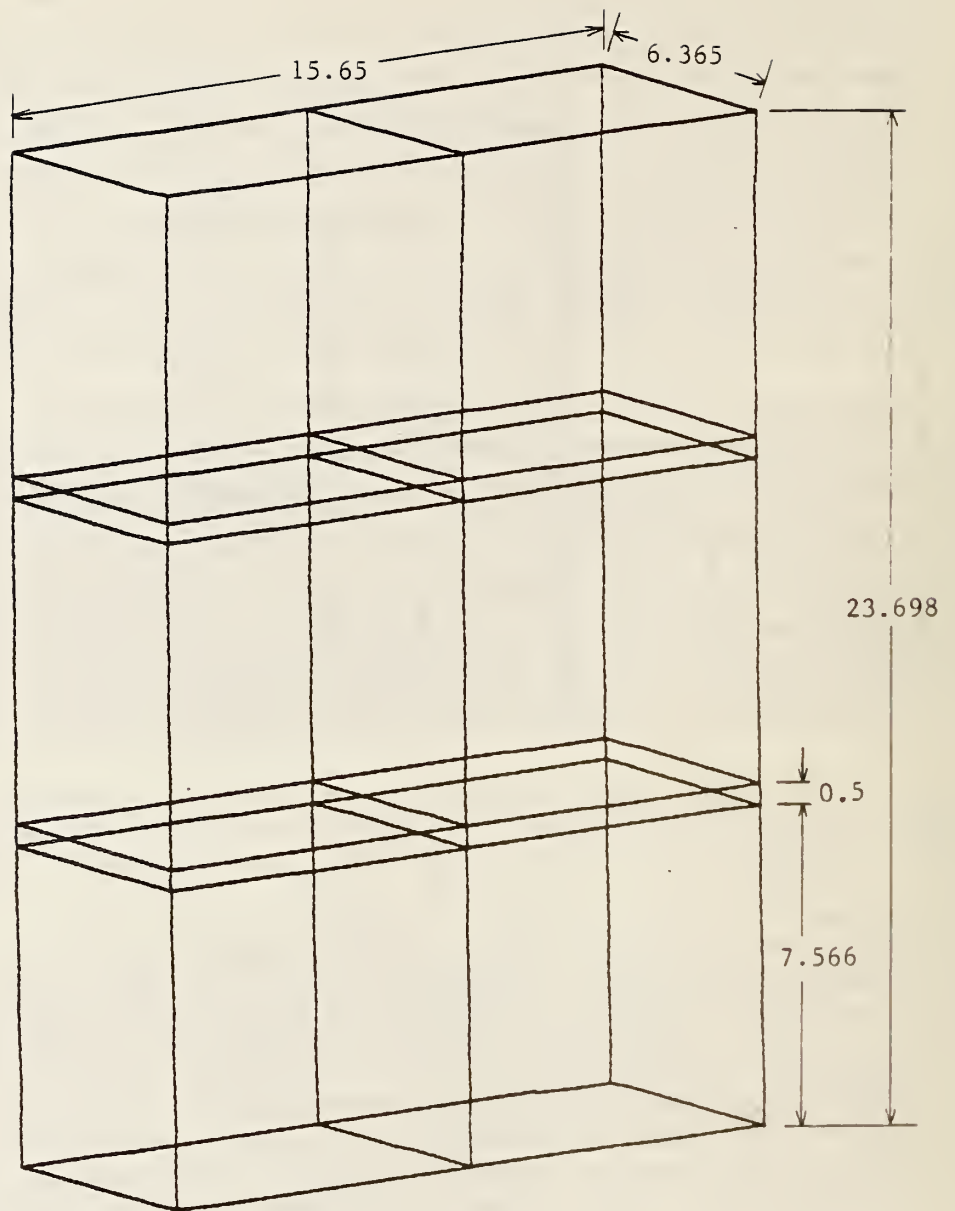


Figure A.2 Finite element prism dimensions (inches).

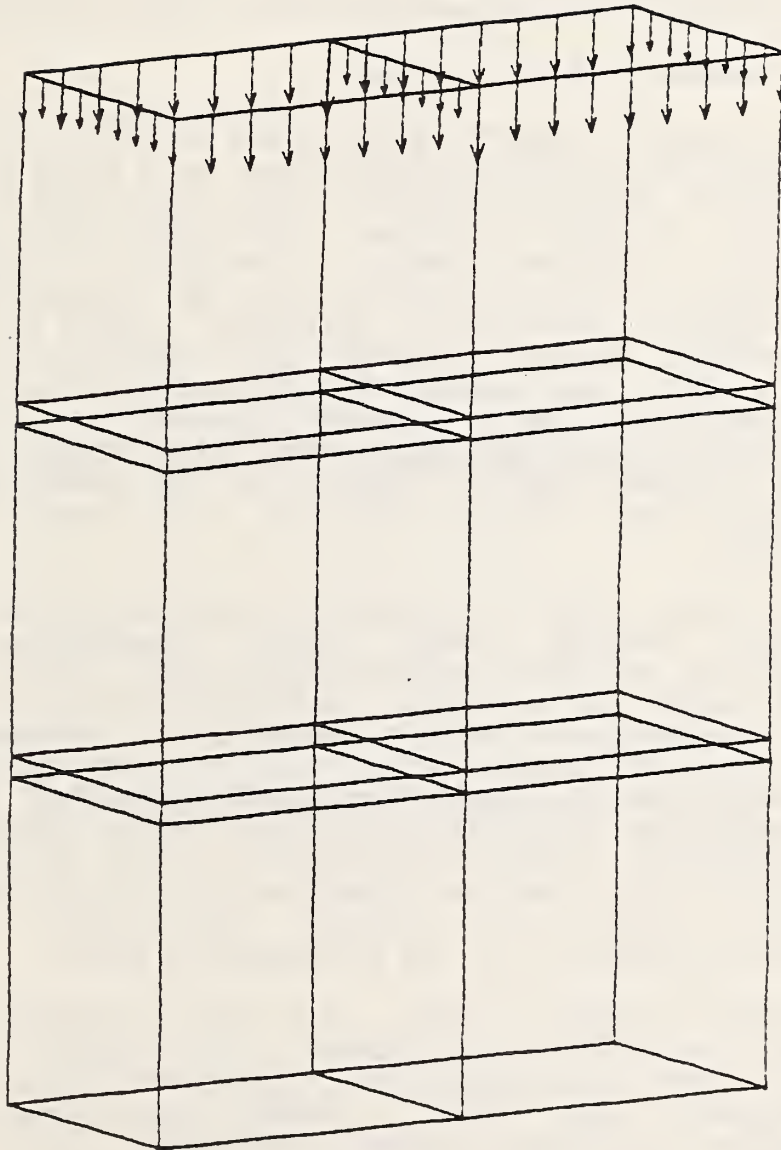


Figure A.3 Loading on finite element prism.

in webs is comparable among blocks of a fully-bedded prism.

Faceshells of full-area-bedded prisms behave in a manner similar to the webs. Vertical stresses are compressive at all points in a faceshell. The major principal stress orientation corresponds to the direction of loading (fig. A.4). The vertical stresses are numerically equivalent among the three blocks of a prism.

A.2.2 Faceshell-Bedded Prisms

Webs of faceshell-bedded prisms have loading configurations which vary depending on whether the block is a middle or an end block. This results in stress distributions that also vary, according to the finite element analysis. Top and bottom blocks have webs that behave like deep beams in bending. Compressive stresses flow from the line of contact with the platen outward to mortar joint supports, with major principal stress orientation ranging from vertical to about forty-five degrees at the mortar joint support. The area bounded by the neutral axis and unsupported edge (unmortared joint between blocks) is in tension and the major principal stress orientation is parallel to the unsupported edge in regions near the edge. At the geometric center of the end block web, both vertical and lateral stresses are compressive.

Middle block webs of faceshell-bedded prisms are stressed indirectly through middle block faceshells. The vertical stresses can not be transmitted directly from the end block webs because there is no mortar between webs of an end and middle block. The analysis predicts compressive stresses that flow from upper faceshell mortar joint out into the plane of the center block web, then to the lower faceshell mortar joint (fig. 4.8). At midheight of a middle block web, from faceshell to mid-web, major principal stress orientation varies from vertical to near horizontal. In the web regions near the unsupported edges, lateral stresses are tensile with major principal stress orientation parallel to the unsupported edge.

In faceshell-bedded prisms, end block faceshells have vertical stresses that differ from those in the middle block faceshell in magnitude and the stress flow is disturbed near the web-faceshell intersection (fig. A.5). These differences were directly accountable to web loading condition. End block webs and faceshells transferred all load into middle block faceshells. Some portion of this stress flowed into the middle block webs, but the result was that middle block faceshells were more highly stressed than were end block faceshells. In end block faceshells, major principal stresses were compressive. In middle block faceshells, the major principal stress orientation was vertical over most of the faceshell. These vertical stresses were compressive and were much larger than lateral stresses, which were tensile.

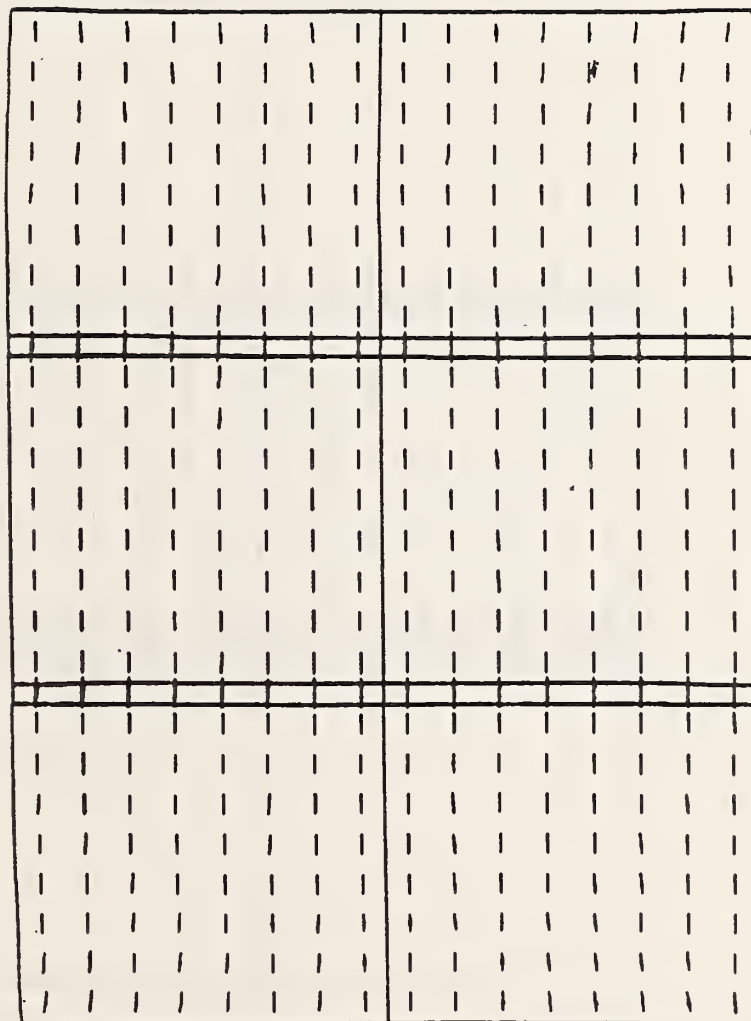


Figure A.4 Stress trajectories in faceshell of a full-area-bedded prism.

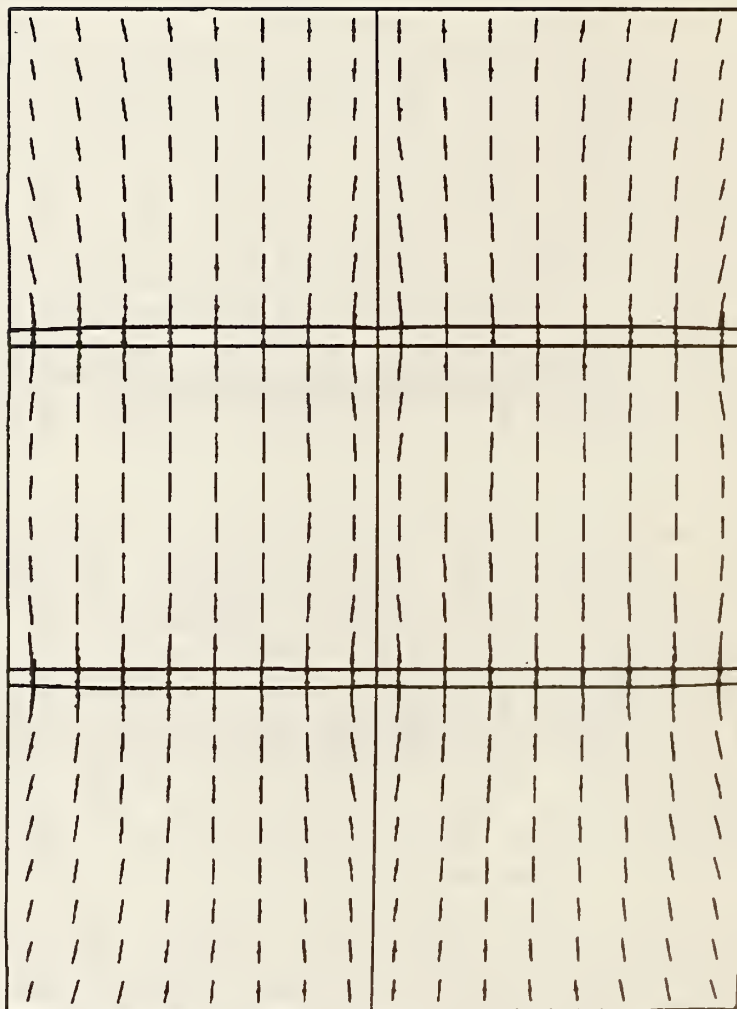


Figure A.5 Stress trajectories in faceshell of a faceshell-bedded prism.

APPENDIX B. PRISM UNIAXIAL STRESS-STRAIN CURVES

Figures B.1 through B.7 contain the uniaxial stress-strain curves for all of the prisms and are grouped by common parameters. The stress is computed by dividing the applied load by the net cross-sectional area of the unit used in the prism. The strain is the average computed strain derived from the two LVDTs' displacement readings. The displacement of each LVDT is divided by the gage length, 16 in., and the two strains are averaged to produce the uniaxial strain value.

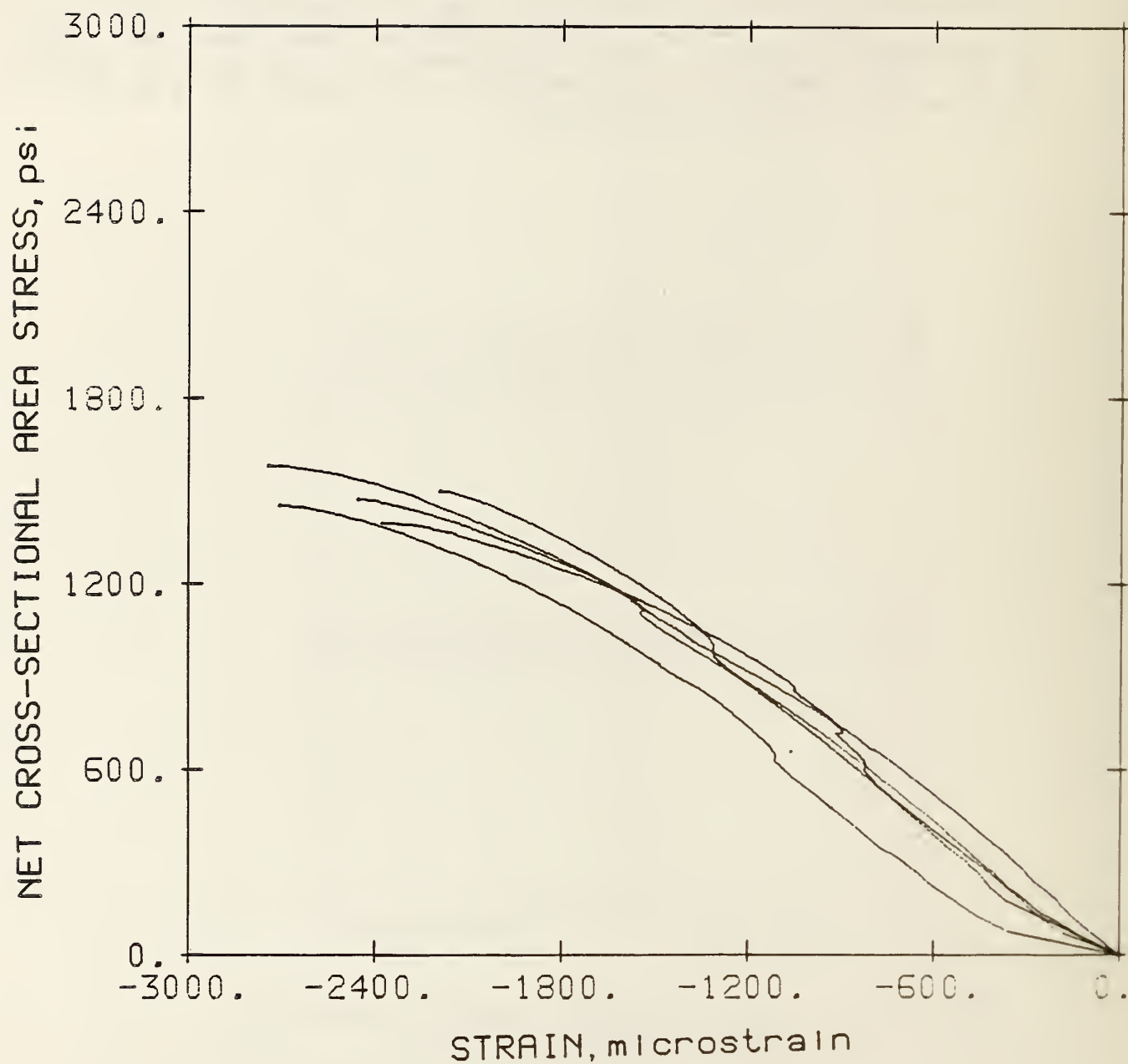


Figure B.1 Stress-strain curves for prisms with low-strength mortar, low-strength block and faceshell bedding.

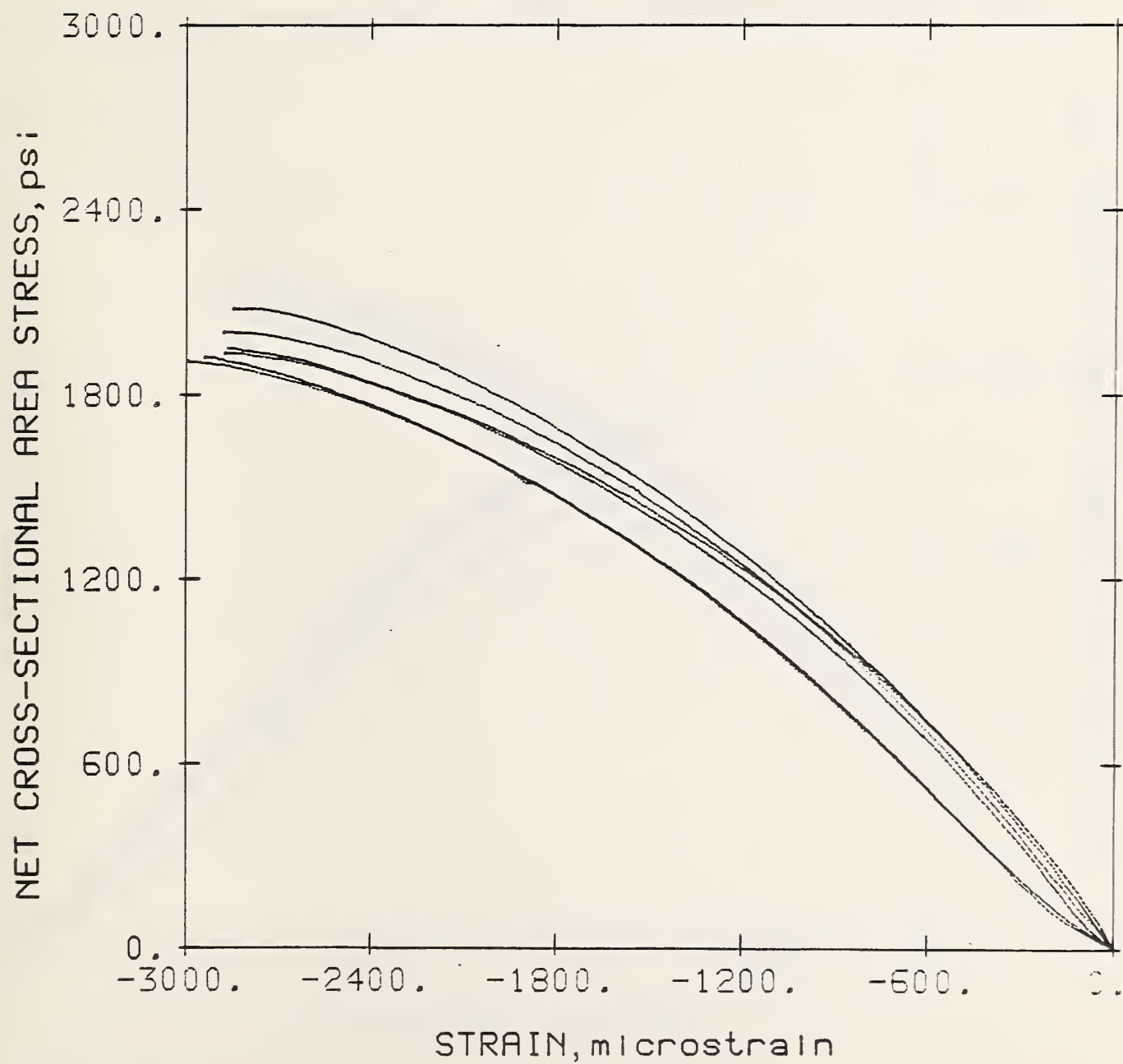


Figure B.2 Stress-strain curves for prisms with low-strength mortar, low-strength block, and full-area bedding.

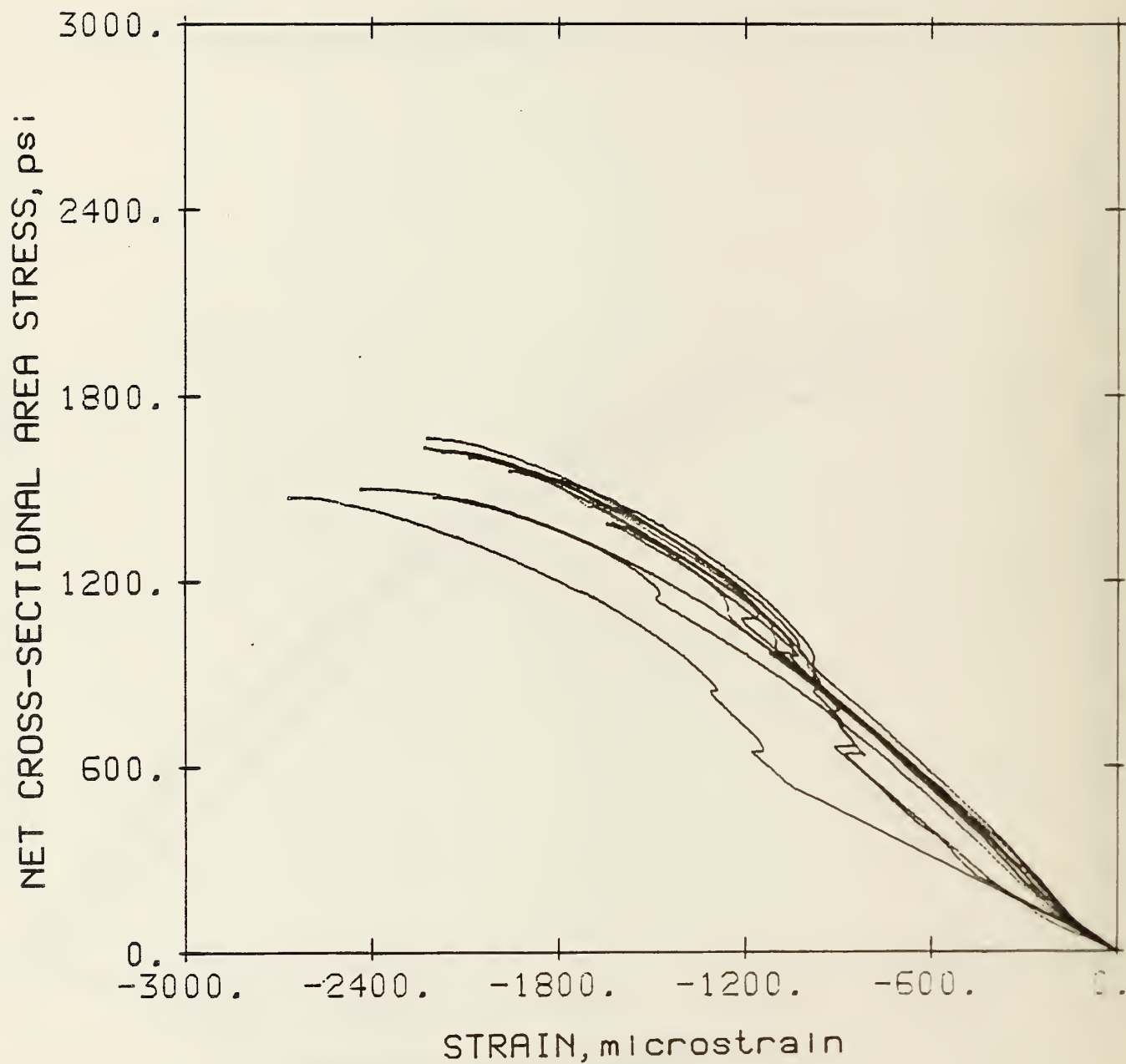


Figure B.3 Stress-strain curves for prisms with high-strength mortar, low-strength block, and faceshell bedding.

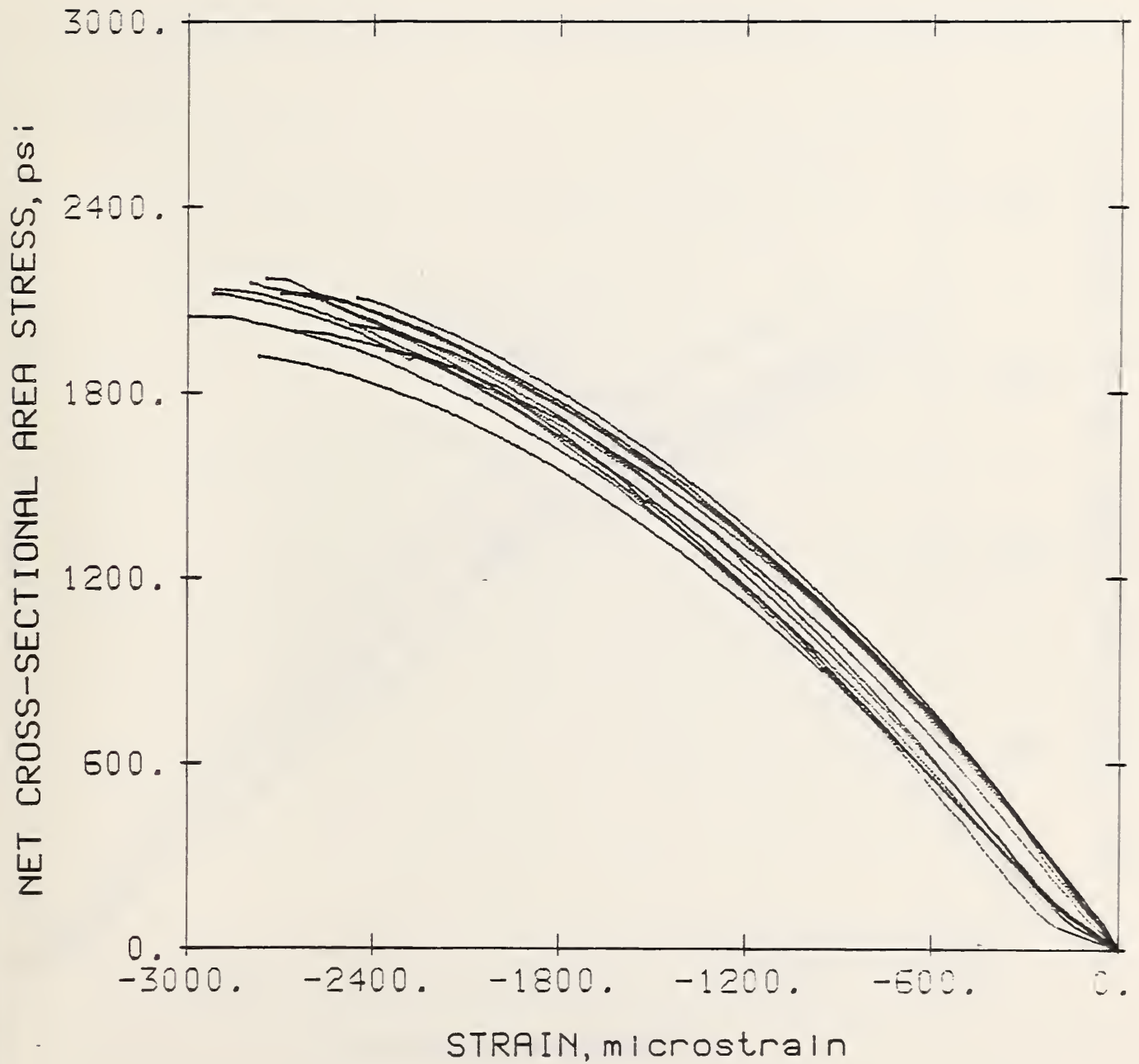


Figure B.4 Stress-strain curves for prisms with high-strength mortar, low-strength block, and full-area bedding.

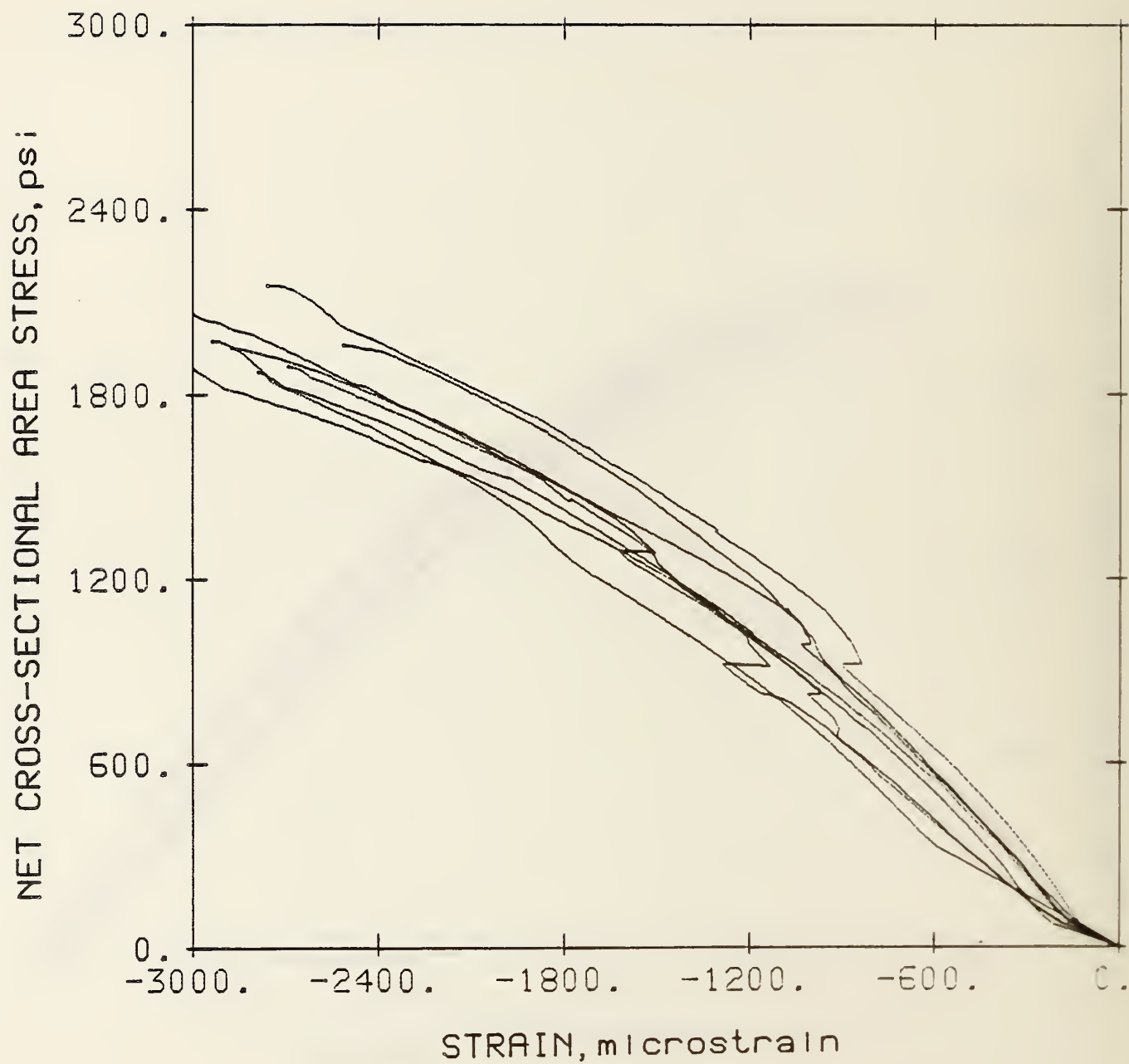


Figure B.5 Stress-strain curves for prisms with low-strength mortar, high-strength block, and faceshell bedding.

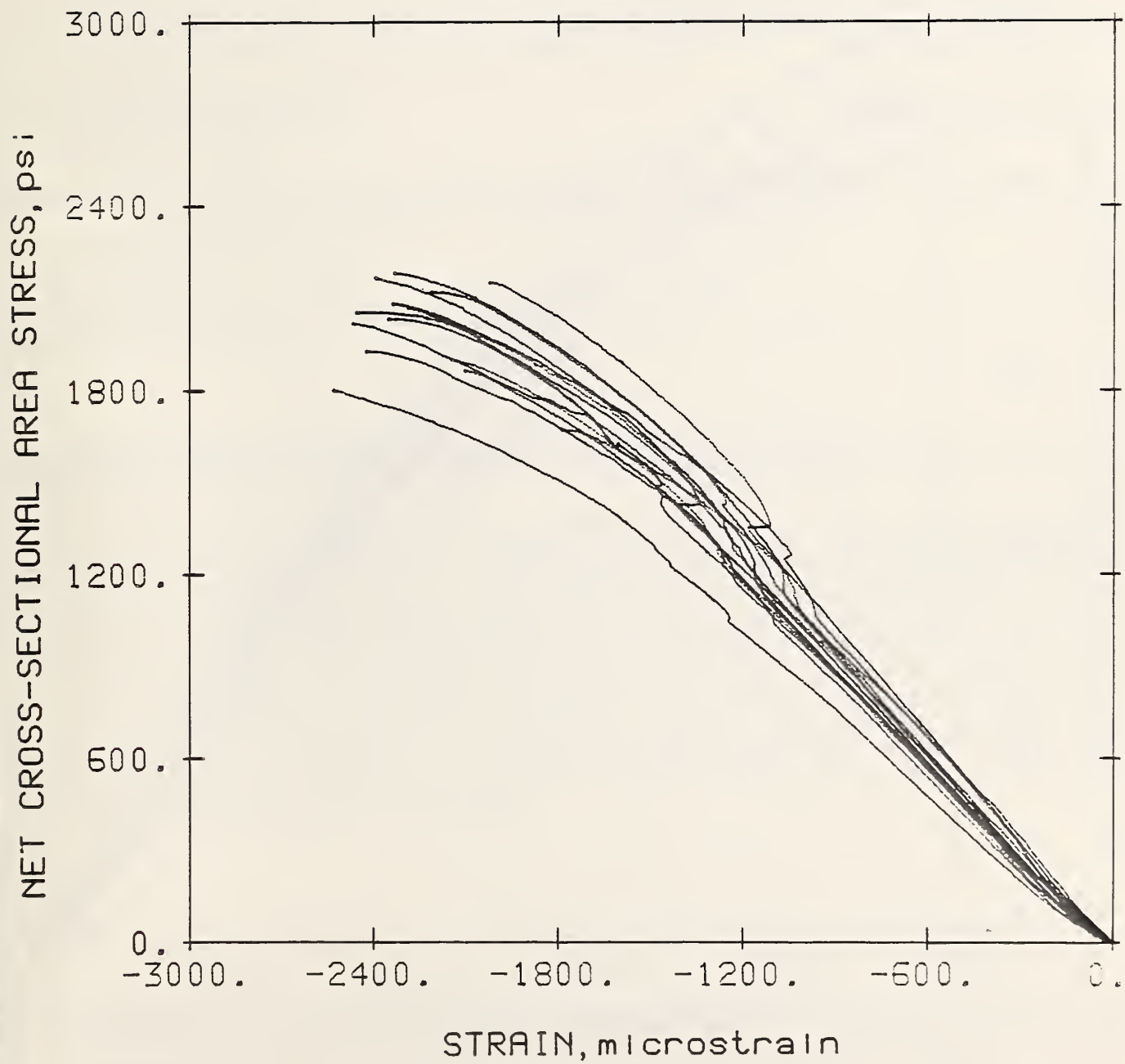


Figure B.6 Stress-strain curves for prisms with high-strength mortar, high-strength block, and faceshell bedding.

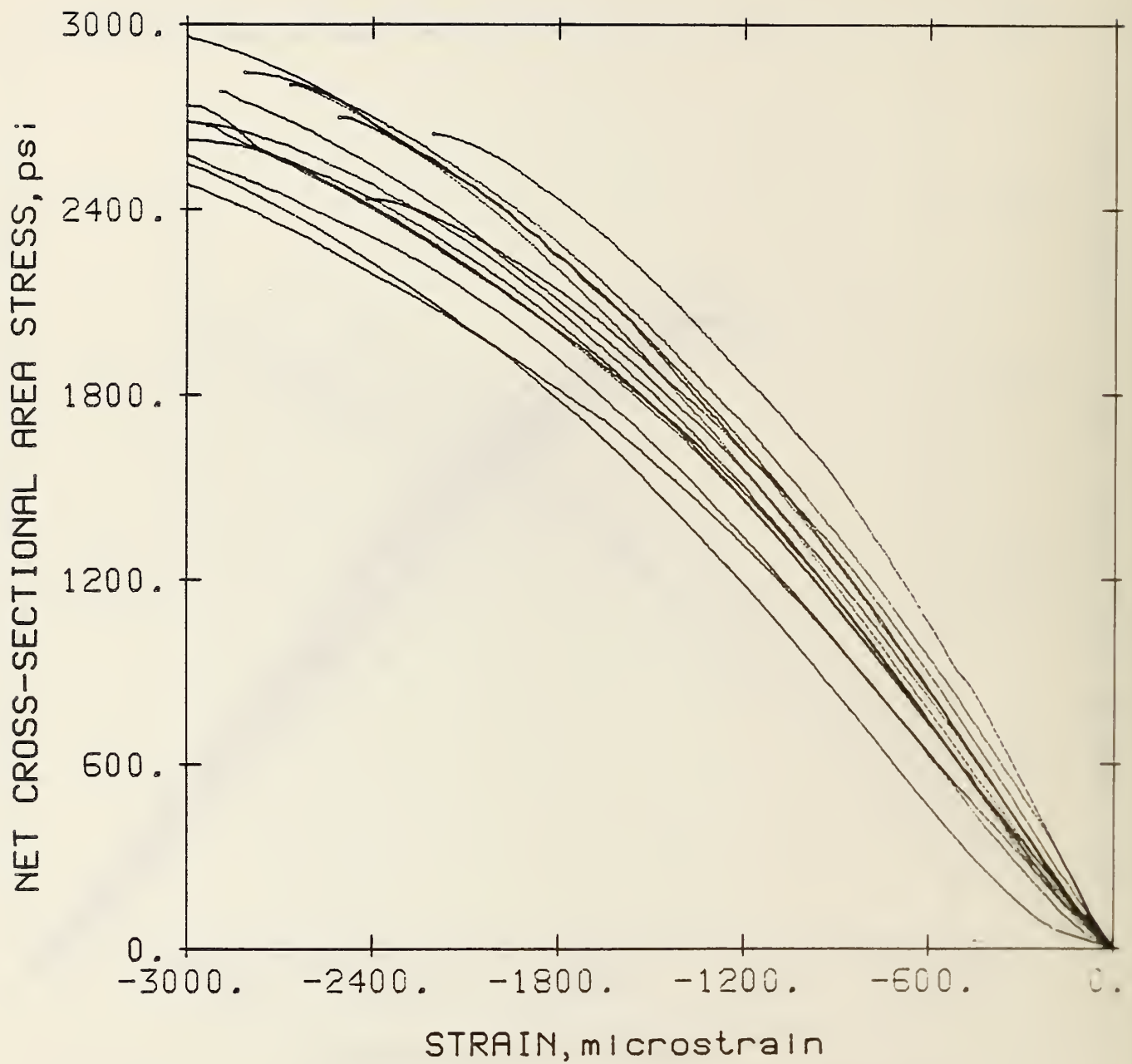


Figure B.7 Stress-strain curves for prisms with high-strength mortar, high-strength block, and full-area bedding.

U.S. DEPT. OF COMM. BIBLIOGRAPHIC DATA SHEET (See instructions)		1. PUBLICATION OR REPORT NO.	2. Performing Organ. Report No.	3. Publication Date
4. TITLE AND SUBTITLE Influence of Mortar Bedding on Masonry Prism Behavior				
5. AUTHOR(S) Patricia Gaynor and Kyle Woodward and Charles Scribner				
6. PERFORMING ORGANIZATION (If joint or other than NBS, see instructions) NATIONAL BUREAU OF STANDARDS DEPARTMENT OF COMMERCE WASHINGTON, D.C. 20234			7. Contract/Grant No.	
			8. Type of Report & Period Covered	
9. SPONSORING ORGANIZATION NAME AND COMPLETE ADDRESS (Street, City, State, ZIP) National Bureau of Standards Department of Commerce Washington, D.C. 20234				
10. SUPPLEMENTARY NOTES <input type="checkbox"/> Document describes a computer program; SF-185, FIPS Software Summary, is attached.				
11. ABSTRACT (A 200-word or less factual summary of most significant information. If document includes a significant bibliography or literature survey, mention it here) The results from compression tests of seventy ungrouted, hollow, concrete block masonry prisms are presented. The prisms are three-high, stack-bonded assemblages. The varied parameters in the investigation include block strength, mortar type, and mortar bedding type (area). The resulting data include the ultimate strength of the prisms and strains measured at various locations on each prims. Major observations of prism behavior are that mortar type has a negligible influence on prism behavior, block strength affects prism ultimate strength in proportion to its own ultimate strength variation, and mortar bedding type significantly affects ultimate strength, its variability, strain distributions, and mode of failure. It is recommended that faceshell bedded prisms not be used as quality control samples for masonry construction because of their disturbed strain fields and higher variability of test data.				
12. KEY WORDS (Six to twelve entries; alphabetical order; capitalize only proper names; and separate key words by semicolons) compression; concrete block; masonry; mortar; prism; ultimate strength				
13. AVAILABILITY <input checked="" type="checkbox"/> Unlimited <input type="checkbox"/> For Official Distribution. Do Not Release to NTIS <input type="checkbox"/> Order From Superintendent of Documents, U.S. Government Printing Office, Washington, D.C. 20402. <input type="checkbox"/> Order From National Technical Information Service (NTIS), Springfield, VA. 22161			14. NO. OF PRINTED PAGES	
			15. Price	

